The Abdus Salam
International Centre for Theoretical Physics

United Nations
Educational, Scientific and
Cultural Organization

IAEA
International Atomic Energy Agency

1929-12

Advanced School on Quantum Monte Carlo Methods in Physics and Chemistry

21 January - 1 February, 2008

Reptation quantum Monte Carlo.

S. Moroni
DEMOCRITOS, SISSA Trieste

Reptation quantum Monte Carlo

Variational projection approach: $\Psi_\beta = e^{-\beta H/2}\Psi_T \rightarrow \Phi_0$

Various algorithms:

- Variational Path Integral
- Path Integral Ground State
- Reptation QMC
- Pure Diffusion Monte Carlo
- .....

Comparison with Diffusion Monte Carlo: Metropolis vs. branching

correlated sampling, derivatives, imaginary-time correlations
population control, mixed estimators

Quantum Monte Carlo Integrals

What integrals do we need to do?
NB They are all un-normalized

$$R \equiv \{\mathbf{r}_1, \mathbf{r}_2, \ldots, \mathbf{r}_N\}$$

$$\hat{P}R \equiv \{\mathbf{r}_{P1}, \mathbf{r}_{P2}, \ldots, \mathbf{r}_{PN}\}$$

$$\left\langle \hat{O} \right\rangle = \frac{\int dR \pi(R) O(R)}{\int dR \pi(R)}$$

METHOD	$\pi(\mathrm{R})$
Classical MC	$\exp\left(-\beta V(R)\right)$
Variational MC	$\left\|\Psi_T(R)\right\|^2 = \left\|\det(R)\right\|^2 e^{-2U(R)}$
Diffusion MC	$\Psi_T(R)\left\langle R\left\|e^{-\tau H}\right\|R'\right\rangle \Psi_T(R')^{-1}$
Reptation MC	$\Psi_T(R_0)\left\langle R_0\left\|e^{-\tau H}\right\|R_1\right\rangle\left\langle R_1\left\|e^{-\tau H}\right\|R_2\right\rangle \ldots \left\langle R_{p-1}\left\|e^{-\tau H}\right\|R_p\right\rangle \Psi_T(R_p)$
Path Integral MC	$\left\langle R_0\left\|e^{-\tau H}\right\|R_1\right\rangle\left\langle R_1\left\|e^{-\tau H}\right\|R_2\right\rangle \ldots \left\langle R_{p-1}\left\|e^{-\tau H}\right\|R_p\right\rangle\left\langle R_{p-1}\left\|e^{-\tau H}\right\|\hat{P}R_0\right\rangle$

Variational projection approach

$T = 0$

We want to calculate quantities such as

$$\langle O \rangle_\beta = \langle \Psi_\beta | \hat{O} | \Psi_\beta \rangle / \langle \Psi_\beta | \Psi_\beta \rangle \,, \quad \text{where} \quad |\Psi_\beta\rangle = e^{-\beta H/2} |\Psi_T\rangle,$$

because $|\Psi_\beta\rangle \underset{\beta \to \infty}{\longrightarrow} |\Phi_0\rangle$ is better than the trial function $|\Psi_T\rangle$.

$$\left(|\Psi_\beta\rangle = \sum_i \langle \Phi_i | \Psi_T \rangle e^{-\beta E_i/2} |\Phi_i\rangle \right)$$

- projection because of $e^{-\beta H}$
- obviously variational: $E_\beta = \langle \Psi_\beta | H | \Psi_\beta \rangle / \langle \Psi_\beta | \Psi_\beta \rangle \geq E_0$
- convergence is monotonic: $-\frac{\partial}{\partial \beta} E_\beta = \langle (H - E_\beta)^2 \rangle > 0$

Trotter breakup: $e^{-\beta H} = \left(e^{-\tau H}\right)^p$ $\tau = \beta/p$ time step

$$\langle O\rangle_\beta = \langle\Psi_\beta|\hat{O}|\Psi_\beta\rangle / \langle\Psi_\beta|\Psi_\beta\rangle$$

$$= \int dX \langle\Psi_T|R_0\rangle\langle R_0|e^{-\tau H}|R_1\rangle \cdots$$

$$\times\langle R_{p/2-1}|e^{-\tau H}|R_{p/2}\rangle O(R_{p/2})\langle R_{p/2}|e^{-\tau H}|R_{p/2+1}\rangle \cdots$$

$$\times\langle R_{p-1}|e^{-\tau H}|R_p\rangle\langle R_p|\Psi_T\rangle \ / \langle\Psi_\beta|\Psi_\beta\rangle$$

$$\simeq \frac{\int dX \pi(X) O(R_{p/2})}{\int dX \pi(X)}$$

$X = \{R_0, \ldots, R_p\}$ is the path

a short time approximation for $\langle R|e^{-\tau H}|R'\rangle$
gives an explicit expression for $\pi(X)$

Trotter breakup: $e^{-\beta H} = \left(e^{-\beta\tau}\right)^p$ $\tau = \beta/p$ time step

$$\langle O\rangle_\beta = \langle\Psi_\beta|\hat{O}|\Psi_\beta\rangle / \langle\Psi_\beta|\Psi_\beta\rangle$$

$$= \int dX \langle\Psi_T|R_0\rangle\langle R_0|e^{-\tau H}|R_1\rangle\cdots$$

$$\times\langle R_{p/2-1}|e^{-\tau H}|R_{p/2}\rangle O(R_{p/2})\langle R_{p/2}|e^{-\tau H}|R_{p/2+1}\rangle\cdots$$

$$\times\langle R_{p-1}|e^{-\tau H}|R_p\rangle\langle R_p|\Psi_T\rangle \Big/ \langle\Psi_\beta|\Psi_\beta\rangle$$

$$\simeq \frac{\int dX\pi(X)O(R_{p/2})}{\int dX\pi(X)}$$

$X = \{R_0,\ldots,R_p\}$ is the path

a short time approximation for $\langle R|e^{-\tau H}|R'\rangle$
gives an explicit expression for $\pi(X)$

PIMC has no trial functions

Trotter breakup: $e^{-\beta H} = \left(e^{-\beta\tau}\right)^p$ $\tau = \beta/p$ time step

$$\langle O\rangle_\beta = \langle\Psi_\beta|\hat{O}|\Psi_\beta\rangle / \langle\Psi_\beta|\Psi_\beta\rangle$$

$$= \int dX \langle\Psi_T|R_0\rangle\langle R_0|e^{-\tau H}|R_1\rangle\cdots$$

$$\times\langle R_{p/2-1}|e^{-\tau H}|R_{p/2}\rangle O(R_{p/2})\langle R_{p/2}|e^{-\tau H}|R_{p/2+1}\rangle\cdots$$

$$\times\langle R_{p-1}|e^{-\tau H}|R_p\rangle\langle R_p|\Psi_T\rangle / \langle\Psi_\beta|\Psi_\beta\rangle$$

$$\simeq \frac{\int dX \pi(X) O(R_{p/2})}{\int dX \pi(X)}$$

$X = \{R_0, \ldots, R_p\}$ is the path

a short time approximation for $\langle R|e^{-\tau H}|R'\rangle$
gives an explicit expression for $\pi(X)$

PIMC has no trial functions

PIMC has closed paths, $R_p = PR_0$

Multilevel Metropolis with bisection

"Variational Path Integral" (D. Ceperley, 1995)

"Path Integral Ground State" (K. Schmidt, 2000)

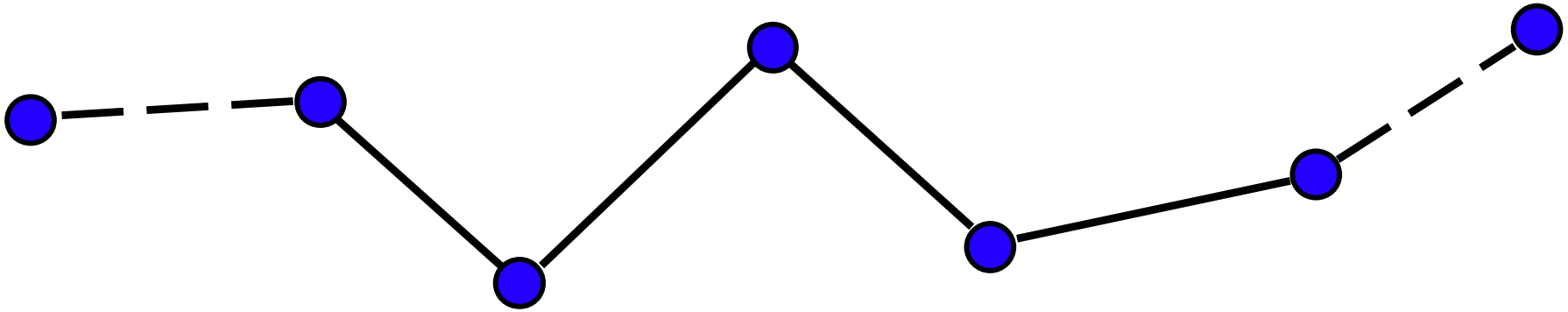

sample the pair action

Multilevel Metropolis with bisection

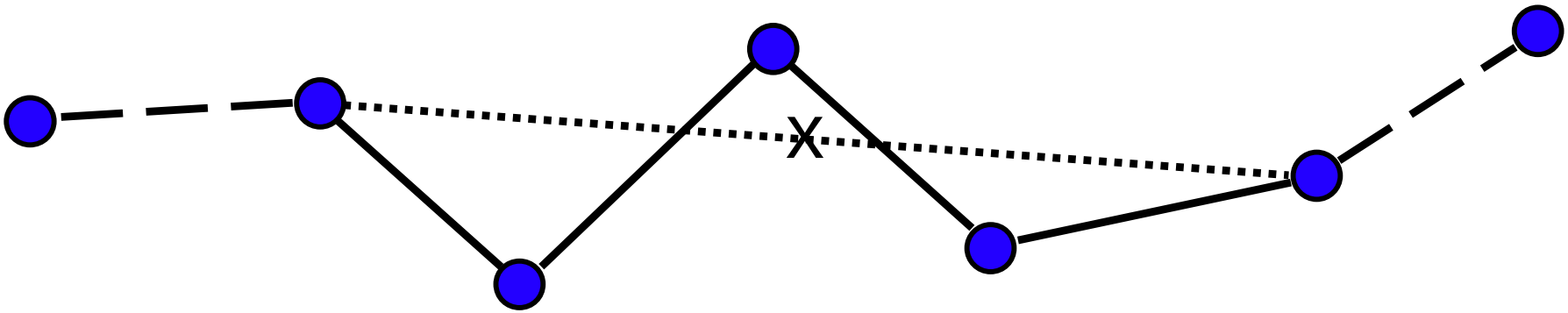

Multilevel Metropolis with bisection

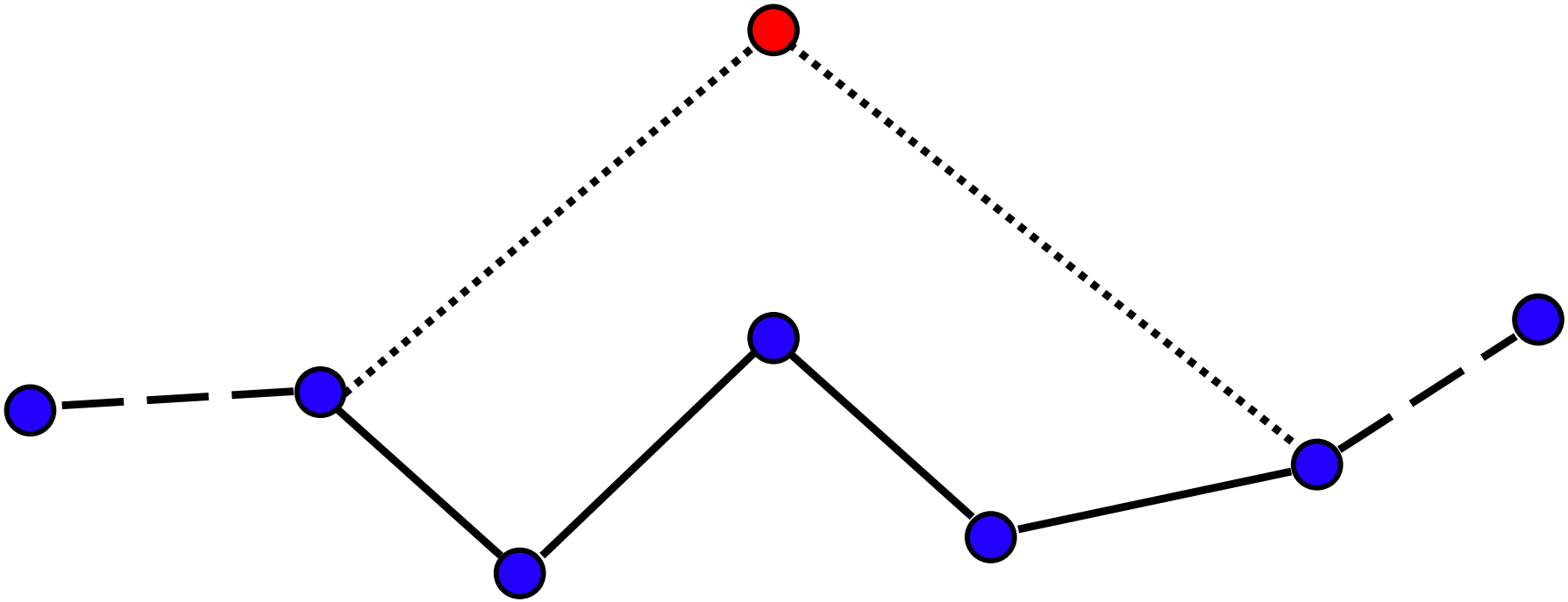

Multilevel Metropolis with bisection

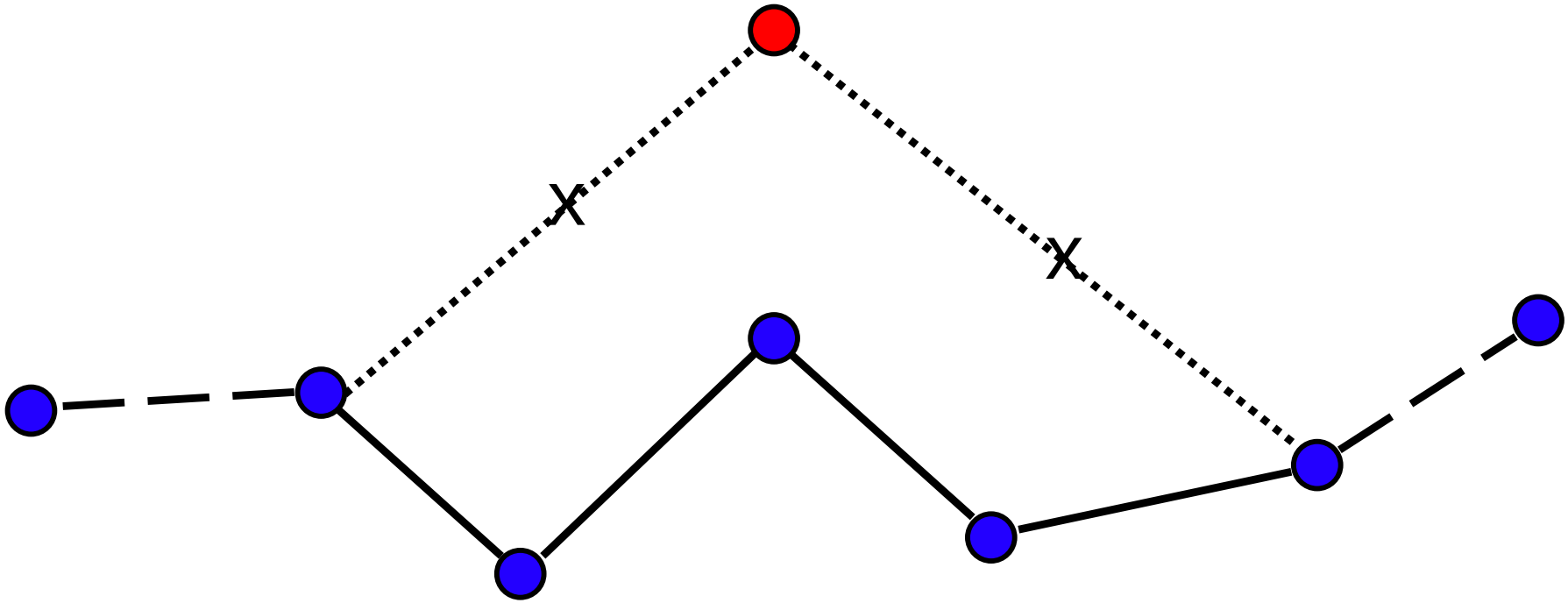

Multilevel Metropolis with bisection

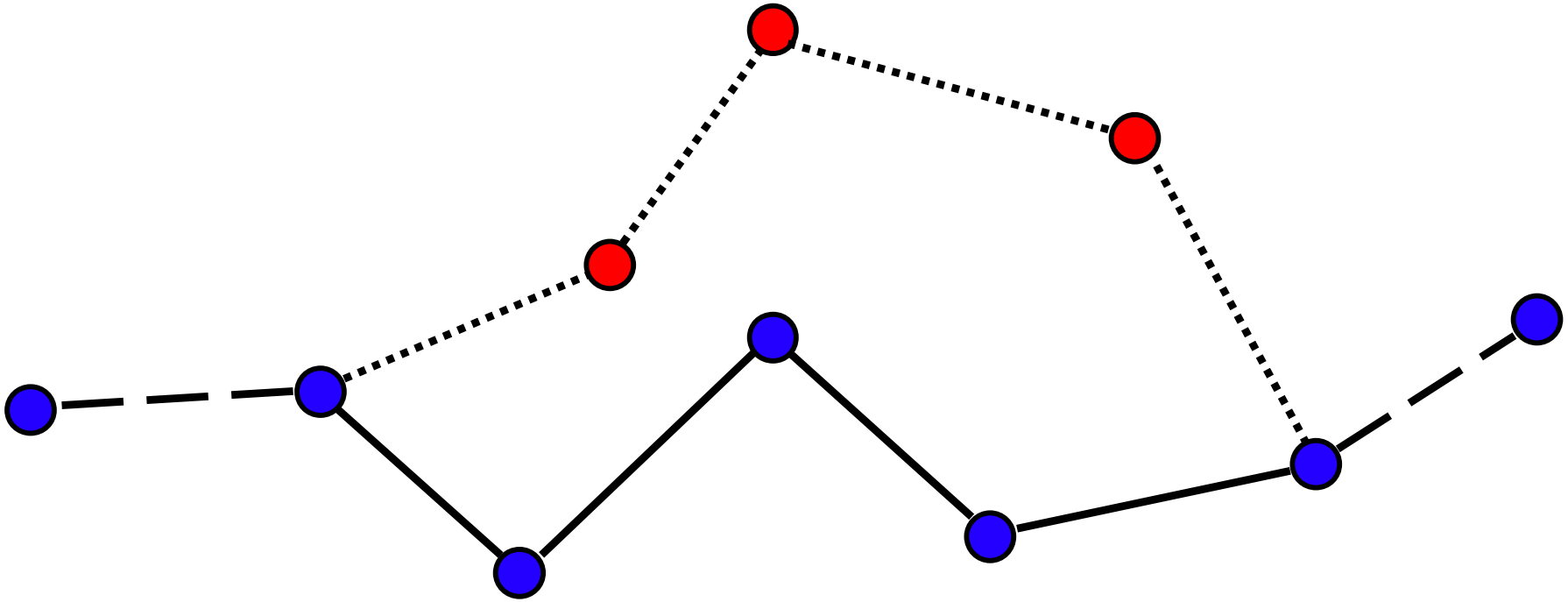

Multilevel Metropolis with bisection

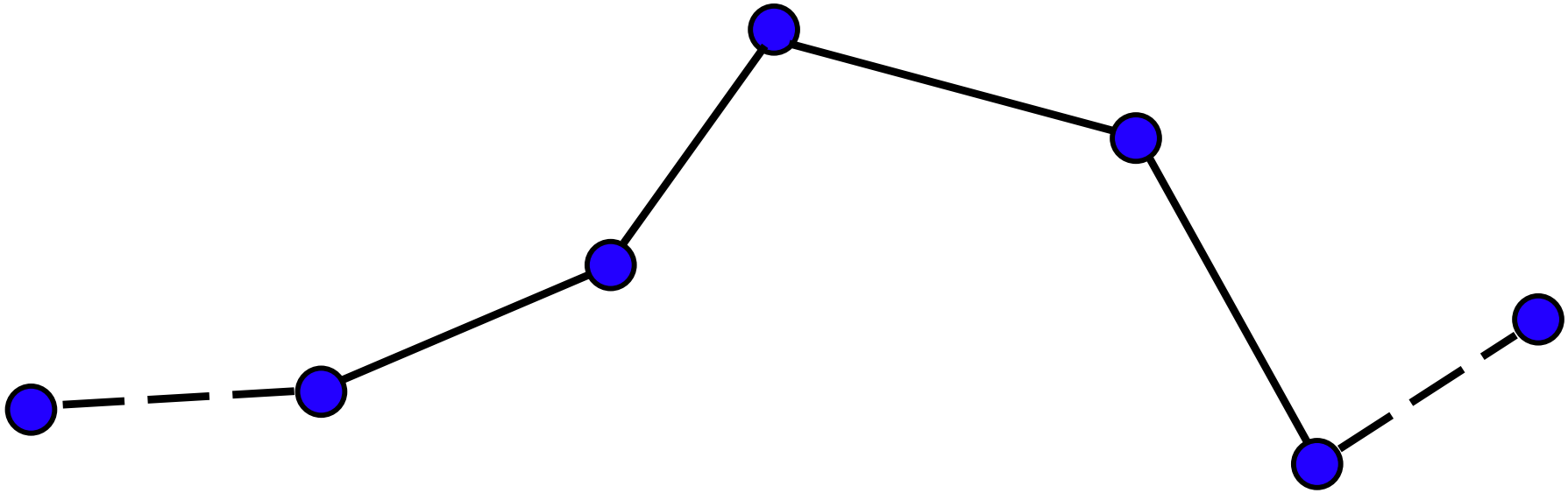

- large local moves without stretching links
- does not use/need importance sampling

(in the DMC sense)

we can introduce importance sampling:

- define $G(R', R, \tau) = \langle R'|e^{-\tau H}|R\rangle$
  and its importance-sampled version $\tilde{G}(R', R, \tau) = \Psi_T(R')\langle R'|e^{-\tau H}|R\rangle/\Psi_T(R)$

- the "pseudo partition function" we use in the simulations is

$$Z_\beta = \int dX \Psi_T(R_0) \prod_{i=1}^{p} G(R_{i-1}, R_i, \tau)\Psi_T(R_p)$$

$$= \int dX \Psi_T(R_0) \frac{G(R_0, R_1)}{\Psi_T(R_1)} \Psi_T(R_1) \ldots \frac{G(R_{p-2}, R_{p-1})}{\Psi_T(R_{p-1})} \Psi_T(R_{p-1}) \frac{G(R_{p-1}, R_p)}{\Psi_T(R_p)} \Psi_T^2(R_p)$$

$$= \int dX \prod_{i=1}^{p} \tilde{G}(R_{i-1}, R_i, \tau)\Psi_T^2(R_p)$$

- the commonly used short time approximation for $\tilde{G}$ is

$$\tilde{G}(R', R, \tau) \simeq e^{-(R'-R-2\lambda\tau V(R))^2/4\lambda\tau} e^{-\tau[E_L(R')+E_L(R)]/2}$$

- for fermions the importance-sampled $\tilde{G}$ enforces the fixed-node constraint

Reptation

"Reptation quantum Monte Carlo" (S. Baroni and SM, 1999)

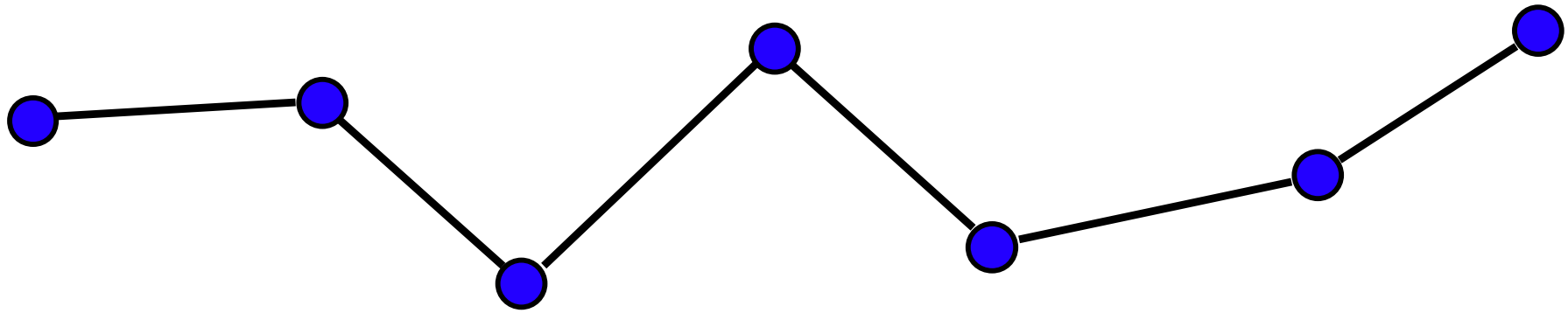

sample $\tilde{\pi}_\beta(X) = \Psi_T^2(R_0) \prod_i e^{-[R_i - R_{i-1} - 2\lambda\tau V(R_{i-1})]^2/4\lambda\tau}$

$\times e^{-\tau[E_L(R_i)+E_L(R_{i-1})]/2}$

Reptation

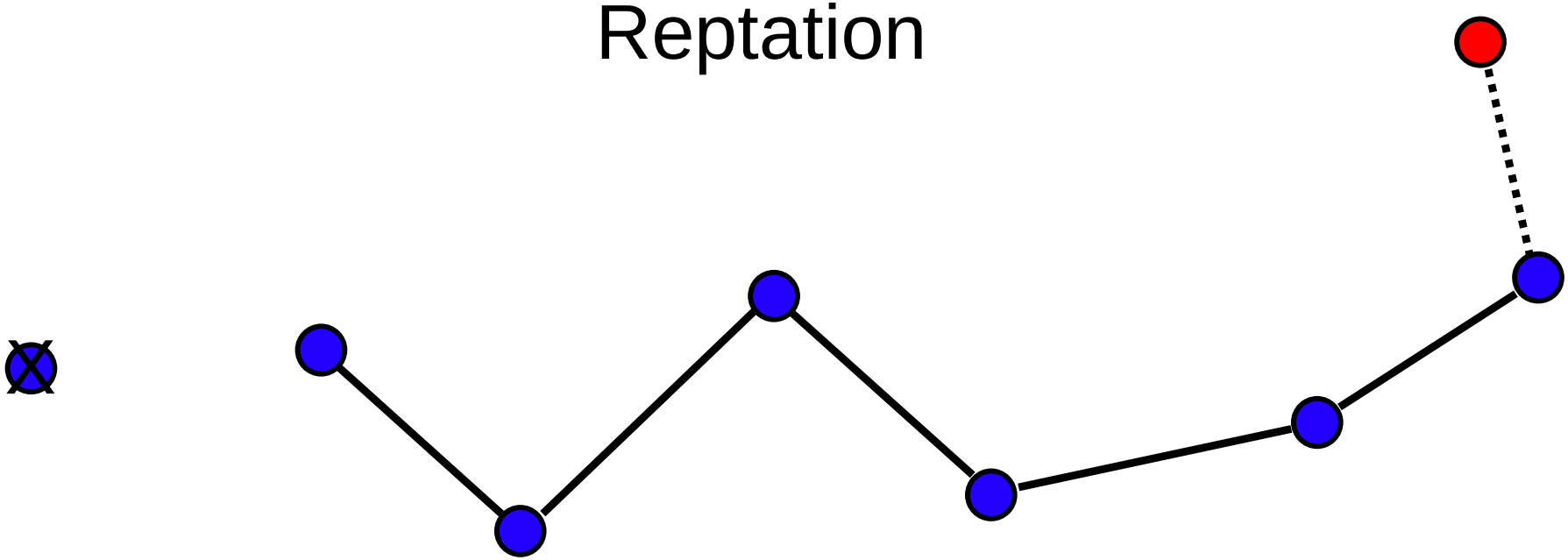

- choose an end of the path, either { randomly, or changing upon rejection *
- move with probability $e^{-[R_{p+1}-R_p-2\lambda\tau V(R_p)]^2/4\lambda\tau}$
- accept with probability $p = \min\left\{1, e^{-\tau(E_L^{\text{head}}-E_L^{\text{tail}})}\right\}$

* “bounce algorithm”, Pierleoni and Ceperley 2005

Reptation

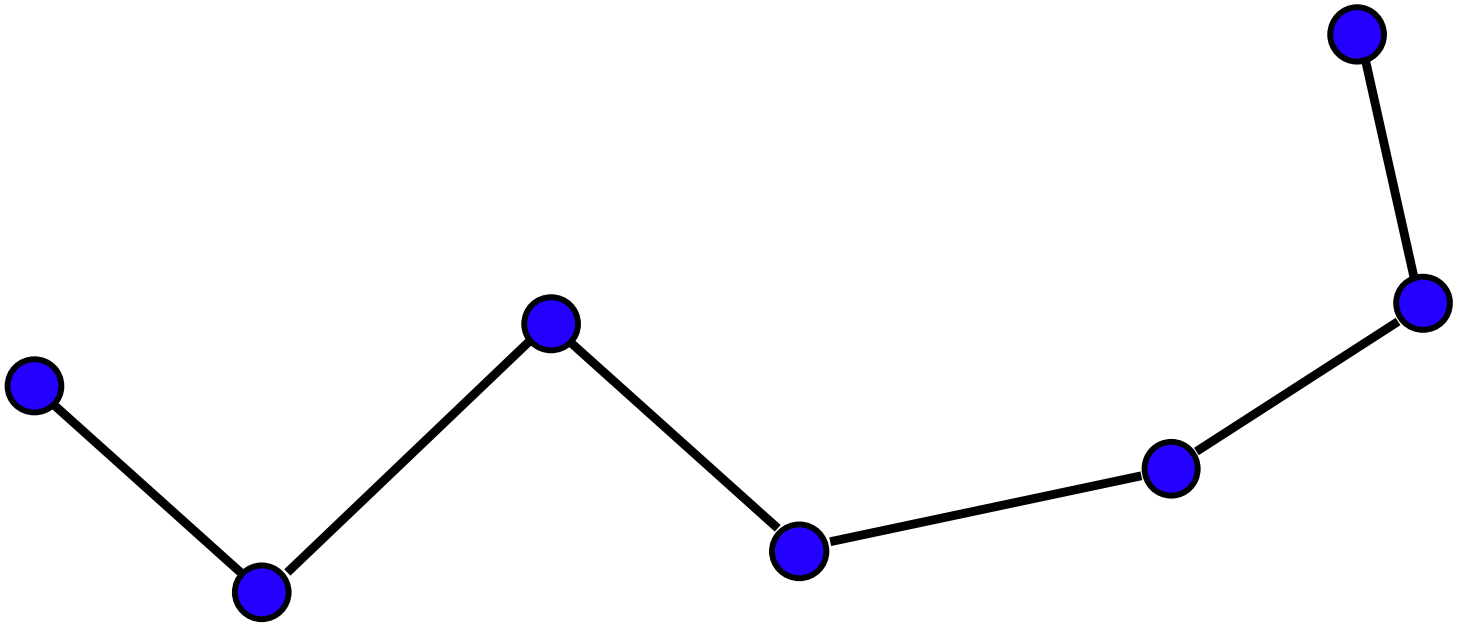

high acceptance rate even for global moves

if the local energy is smooth (uses importance sampling)

Reptation

" accept with probability $p = \min\left\{1, e^{-\tau(E_L^{\text{head}} - E_L^{\text{tail}})}\right\}$ "

more precisely:

a priori transition probability $T(X \to X') = e^{-[R_{p+1} - R_p - 2\lambda\tau V(R_p)]^2/4\lambda\tau}$

for the reverse move $T(X' \to X) = e^{-[R_0 - R_1 - 2\lambda\tau V(R_1)]^2/4\lambda\tau}$

$$\frac{\tilde{\pi}(X')}{\tilde{\pi}(X)} \frac{T(X' \to X)}{T(X \to X')} = e^{-\tau[E_L(R_{p+1}) + E_L(R_p) - E_L(R_1) - E_L(R_0)]/2} \times \frac{\Psi_T^2(R_1)}{\Psi_T^2(R_0)} \frac{e^{-[R_0 - R_1 - 2\lambda\tau V(R_1)]^2/4\lambda\tau}}{e^{-[R_1 - R_0 - 2\lambda\tau V(R_0)]^2/4\lambda\tau}}$$

this factor is nonzero because of the time step error

Langevin + weights

"Pure Diffusion Monte Carlo" (Caffarel and Claverie, 1988)

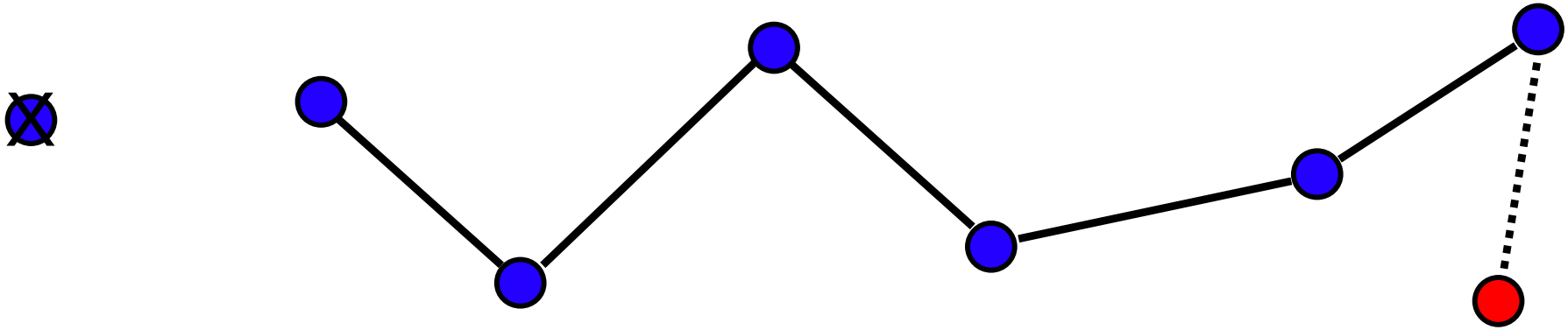

- move with probability $e^{-[R_{p+1}-R_p-2\lambda\tau V(R_p)]^2/4\lambda\tau}$ (Langevin)
- never change direction
- weight averages with $W = \exp\left(-\tau \sum_{\text{path}} E_L(R_i)\right)$

useful for small systems

Calculating properties

What is the distribution of individual time slices along the path?

integrate over all the other time slices:

$$P(R_0) = \int dR_1 \ldots dR_p \pi(X)$$
$$= \langle \Psi_T | R_0 \rangle \langle R_0 | e^{-\beta H} | \Psi_T \rangle \simeq \Psi_T(R_0)\Phi_0(R_0)$$

- the end(s) of the path sample the “mixed distribution”

For an inner slice (say $j = p/2$):

$$P(R_j) = \langle \Psi_T | e^{-\beta H/2} | R_j \rangle \langle R_j | e^{-\beta H/2} | \Psi_T \rangle \simeq \Phi_0^2(R_j)$$

- the inner slices sample the “pure distribution”

The mixed estimate $O_{\mathrm{mix}} = \langle \Psi_T | \hat{O} | \Phi_0 \rangle / \langle \Psi_T | \Phi_0 \rangle$ is unbiased only if $[O, H] = 0$. This is a problem in Diffusion Monte Carlo

Calculating properties

Sarsa, Schmidt, Magro 2000

	E/N (K)	T/N (K)
VMC[a]	−7.0000(54)	14.2185(78)
GFMC[a]	−7.292(3)	14.030(21)
Extrapolated		13.842(50)
PIGS	−7.318(38)	14.390(60)

- With DMC one usually combines the mixed estimate

$$O_{\rm mix} = \langle \Psi_T | O | \Phi_0 \rangle / \langle \Psi_T | \Phi_0 \rangle$$

and the variational estimate

$$O_{\rm var} = \langle \Psi_T | O | \Psi_T \rangle / \langle \Psi_T | \Psi_T \rangle$$

to get “extrapolated estimates”

$$O_{\rm ext} = 2O_{\rm mix} - O_{\rm var} \quad \text{or} \quad O_{\rm ext} = O_{\rm mix}^2 / O_{\rm var}$$

whose error is quadratic in the error of the trial function. In this example O_{ext} is worse than both O_{mix} and O_{var} .

- This PIGS calculation uses a simple Jastrow for both the liquid and the solid. DMC would need a Nosanow term for the solid, so it is more trial-function dependent.

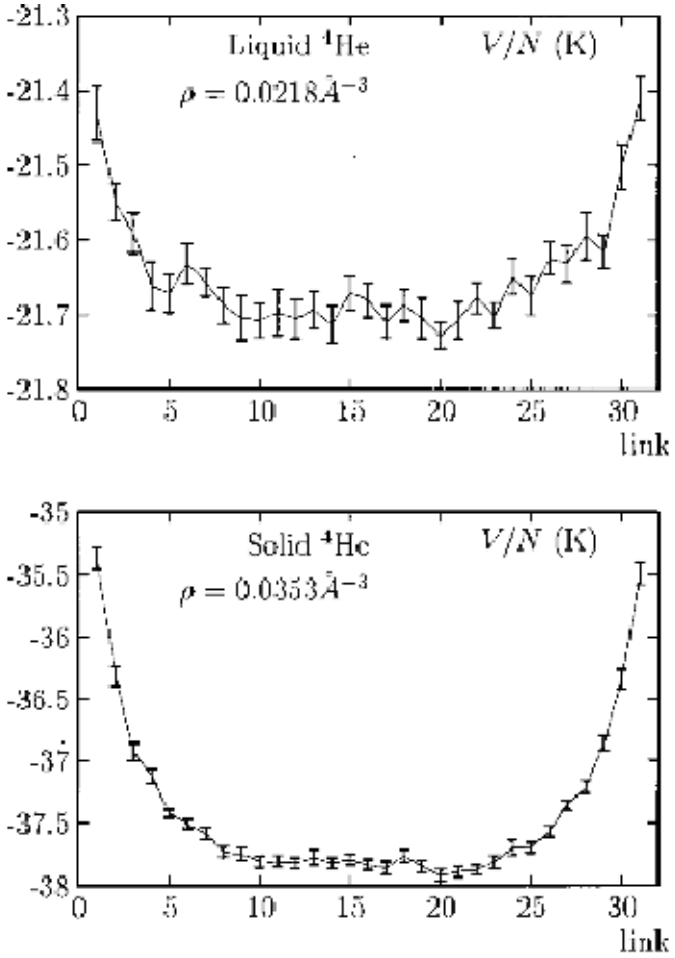

potential energy as a function of the link in the PIGS calculation

Calculating properties

- For the energy, use the mixed estimator to exploit the zero-variance property of the local energy:

$$E_\beta = \int dX \frac{1}{2} \left[E_L(R_0) + E_L(R_p) \right] \pi(X)$$

- For other quantities, use the middle slice(s):

$$O_\beta = \int dX O(R_{p/2}) \pi(X)$$

- Imaginary-time correlation functions:

$$C_{AB}(k\tau) = \int dX A(R_j) B(R_{j+k}) \pi(X)$$

- Correlated sampling and derivatives are just as simple as in Variational Monte Carlo, e.g.:

$$\nabla E_\beta = \int dX \left\{ \nabla E_L(R_0) + \left[E_L(R_0) - E_\beta \right] \nabla \ln \pi(X) \right\} \pi(X)$$

Convergence tests($^4He_3$ - CO_2 cluster, RQMC)

projection time extrapolation

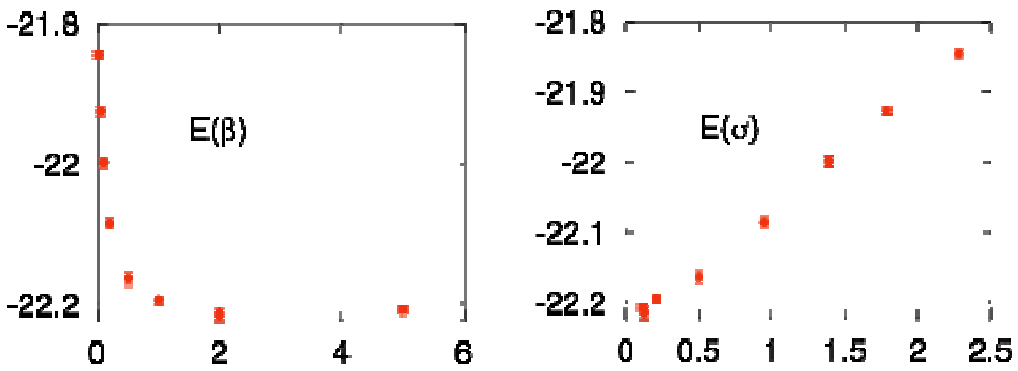

time-step extrapolation

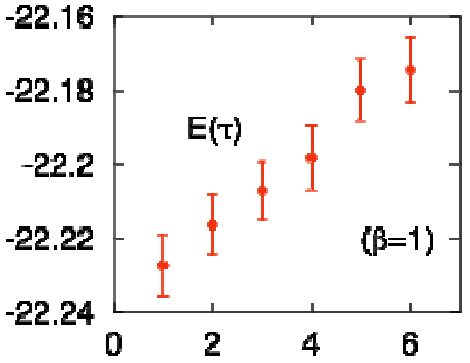

$$\sigma_\beta^2 = \langle (H - \langle H \rangle_\beta)^2 \rangle_\beta$$
$$= \langle E_L(R_0) E_L(R_P) - \langle H \rangle_\beta^2 \rangle_\beta$$

this variance goes to zero for $\beta \to \infty$

extrapolation of the energy to zero variance is easier than to $\beta \to \infty$

path diffusion

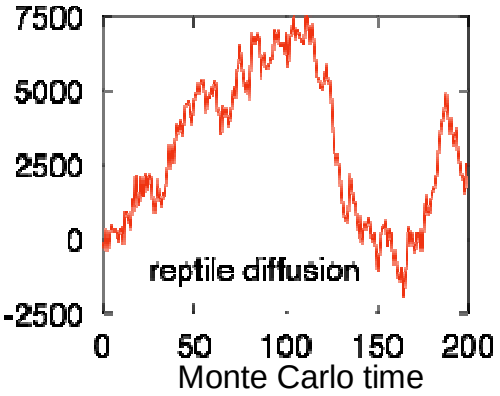

(make sure the path doesn't get stuck)

calculating derivatives of the fixed-node energy:

static linear susceptibility of the 2D electron gas

$$H = H_0 + 2v_k \sum_{i=1}^{N} \cos(\mathbf{k} \cdot \mathbf{r}_i)$$

$$\Delta E = \frac{\chi(k)}{\rho} v_k^2 + \frac{\chi^{(3)}(\mathbf{k}, \mathbf{k}, -\mathbf{k})}{4} v_k^4 + \cdots$$

Susceptibilities are calculated as second derivatives at zero external field using RQMC.

- choice of Ψ_T : nodes from the ground state of non-interacting particles in a cosine potential. α is a variational parameter.

$$H^{(\mathrm{ni})} = H_0^{(\mathrm{ni})} + 2\alpha v_k \sum_i \cos(\mathbf{k}\cdot\mathbf{r}_i) \quad \text{(Mathieu functions)}$$

- short-time approximation to $\langle R|e^{-\tau H}|R'\rangle$:

$$\langle R|e^{-\tau H}|R'\rangle \simeq e^{-(R-R')^2/4\lambda\tau}\left(1-e^{-dd'/\lambda\tau}\right)e^{-\tau[V(R)+V(R')]/2}$$

This is the primitive+nodal action.
The nodal action enforces the fixed-node approximation.
It is obtained solving a 1D particle near an infinite barrier by the method of images.

- estimate the nodal distance by linearizing the trial function: $d \simeq |\Psi_T/\nabla\Psi_T|$

near the nodes the nodal action is better behaved
than the importance-sampled drift-diffusion term

$$\tilde{G}(R',R,\tau) \simeq e^{-(R'-R-2\lambda\tau V(R))^2/4\lambda\tau} e^{-\tau[E_L(R')+E_L(R)]/2}$$

- choice of Ψ_T : nodes from the ground state of non-interacting particles in a cosine potential. α is a variational parameter.

$$H^{(\mathrm{ni})} = H_0^{(\mathrm{ni})} + 2\alpha v_k \sum_i \cos(\mathbf{k}\cdot\mathbf{r}_i)$$ (Mathieu functions)

- short-time approximation to $\langle R|e^{-\tau H}|R'\rangle$:

potential

$$\langle R|e^{-\tau H}|R'\rangle \simeq e^{-(R-R')^2/4\lambda\tau}\left(1-e^{-dd'/\lambda\tau}\right)e^{-\tau[V(R)+V(R')]/2}$$

This is the primitive+nodal action.
The nodal action enforces the fixed-node approximation.
It is obtained solving a 1D particle near an infinite barrier by the method of images.

- estimate the nodal distance by linearizing the trial function: $d \simeq |\Psi_T/\nabla\Psi_T|$

near the nodes the nodal action is better behaved
than the importance-sampled drift-diffusion term

$$\tilde{G}(R',R,\tau) \simeq e^{-(R'-R-2\lambda\tau V(R))^2/4\lambda\tau} e^{-\tau[E_L(R')+E_L(R)]/2}$$

drift velocity

static linear susceptibility of the 2D electron gas

$$H = H_0 + 2v_k \sum_{i=1}^{N} \cos(\mathbf{k}\cdot\mathbf{r}_i)$$

$$\Delta E = \frac{\chi(k)}{\rho} v_k^2 + \frac{\chi^{(3)}(\mathbf{k},\mathbf{k},-\mathbf{k})}{4} v_k^4 + \cdots$$

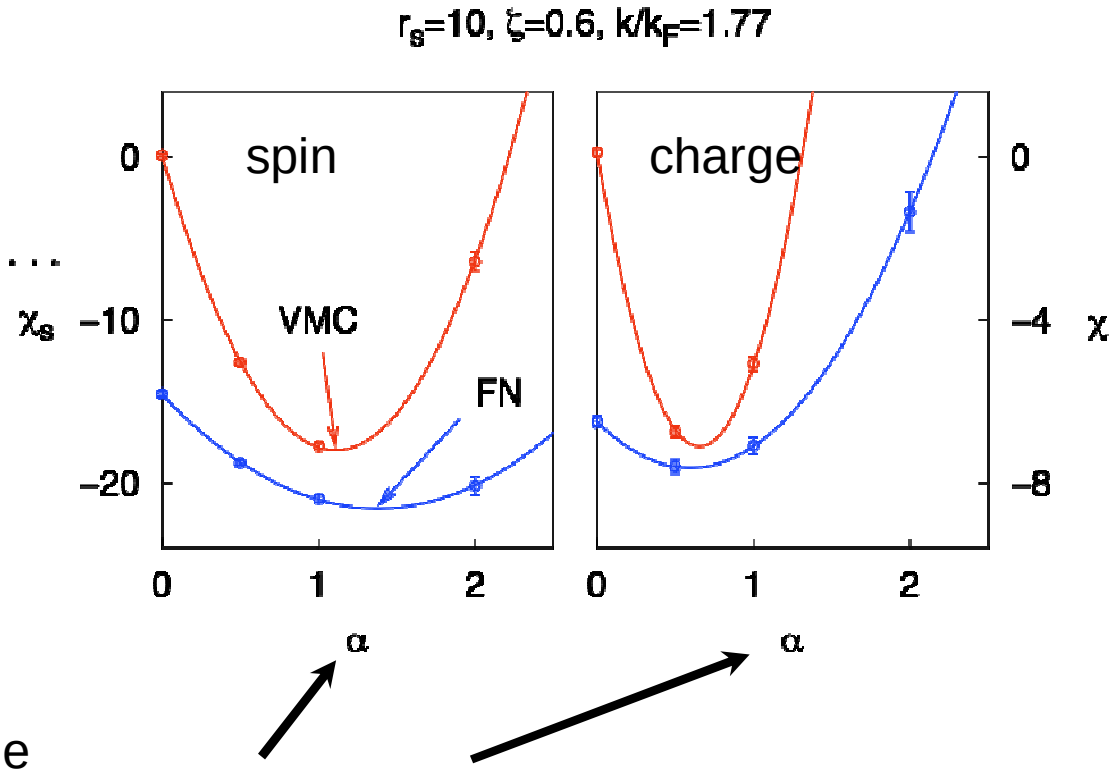

Susceptibilities are calculated as second derivatives at zero external field using RQMC.

The nodal displacement increases the statistical noise, in a way which strongly depends on the fixed-node constraint imposed by the Green's function. The "nodal action" by far outperforms the "drift diffusion".

A parameter in the trial function that controls the nodal displacement induced by the external potential. A zero value means no displacement, the optimal value is the location of the minimum of the curve.

static linear susceptibility of the 2D electron gas

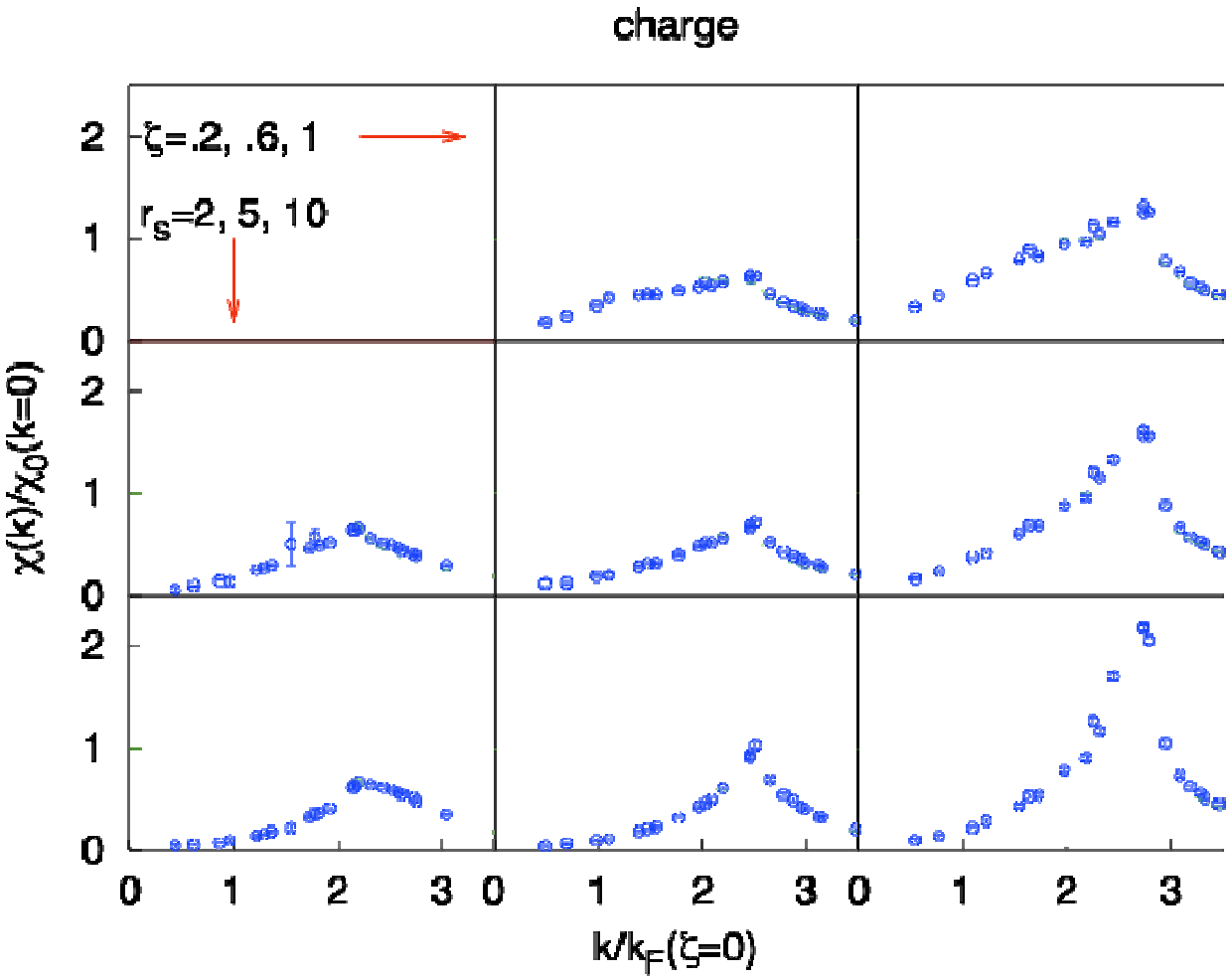

application to electronic structure: forces

cumulant approximation to pair action (Ceperley, 1983)

$$G(R',R,\epsilon) \propto \mathrm{e}^{-(R-R')^2/2\epsilon}\left(1-\mathrm{e}^{-2dd'/\epsilon}\right)\mathrm{e}^{-\sum_{i<j} u(\mathbf{r}_{ij},\mathbf{r}'_{ij},\epsilon)}$$

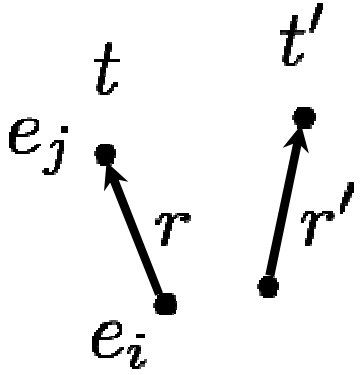

$$s = |r-r'|\,(2\hbar^2\epsilon/\mu)^{-1/2}$$

$$y = (r+r'+|r-r'|)\,(2\hbar^2\epsilon/\mu)^{-1/2}$$

$$\gamma = e_i e_j (2\epsilon\mu/\hbar^2)^{-1/2}$$

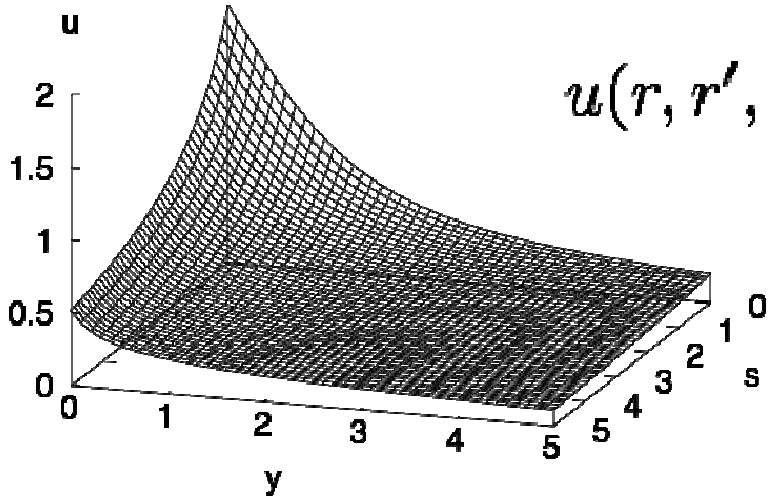

$$u(r,r',\epsilon) = \gamma \int_0^1 d\lambda \frac{1}{y+2s\lambda}\mathrm{erf}\left(\frac{y+2s\lambda}{2[\lambda(1-\lambda)]^{1/2}}\right)$$

one two-dimensional table

hydrogen dimer,

$$\phi(\mathbf{r}) = \mathrm{e}^{-|\mathbf{r}-\mathbf{r}_{H1}|} + \mathrm{e}^{-|\mathbf{r}-\mathbf{r}_{H2}|}$$

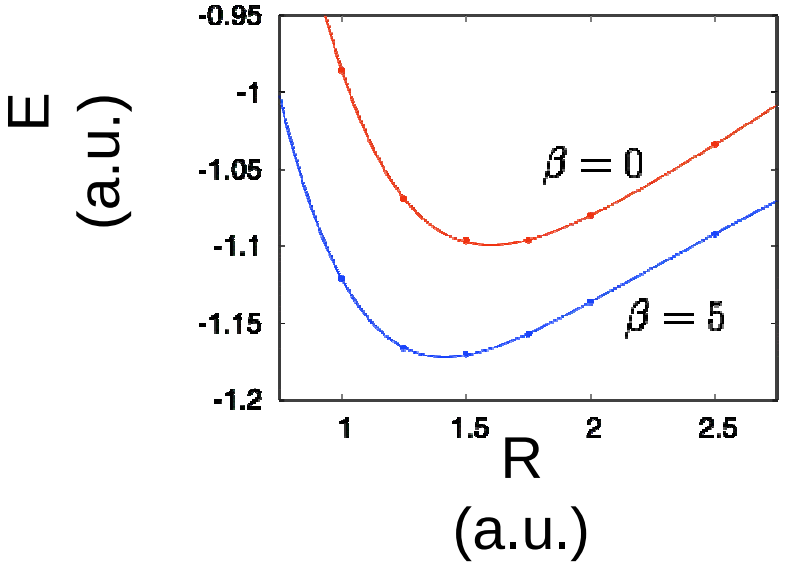

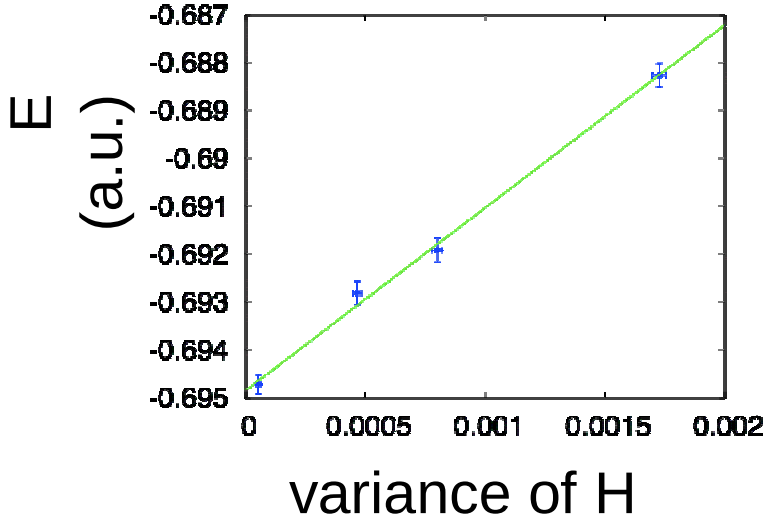

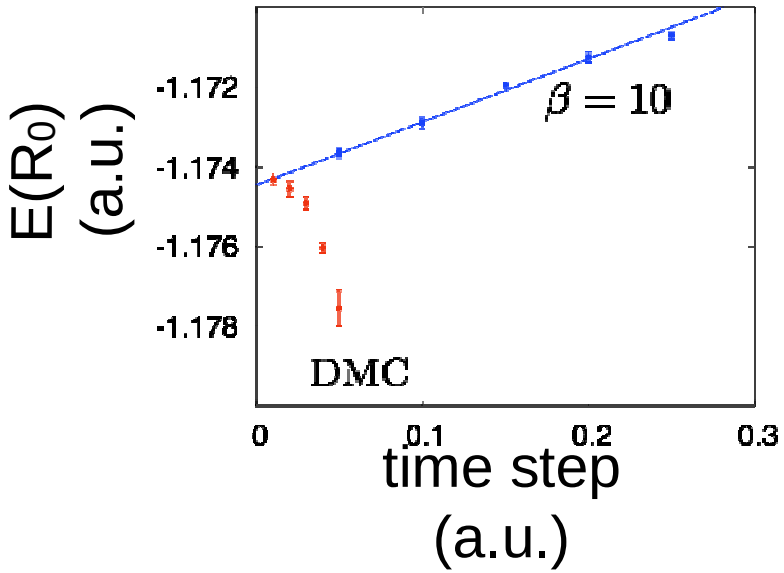

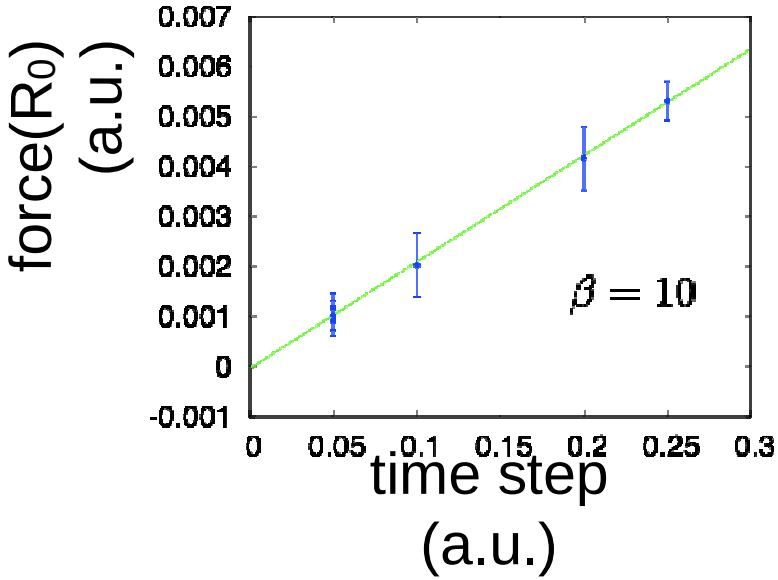

examples of calculations of forces

Assaraf, Caffarel
2003

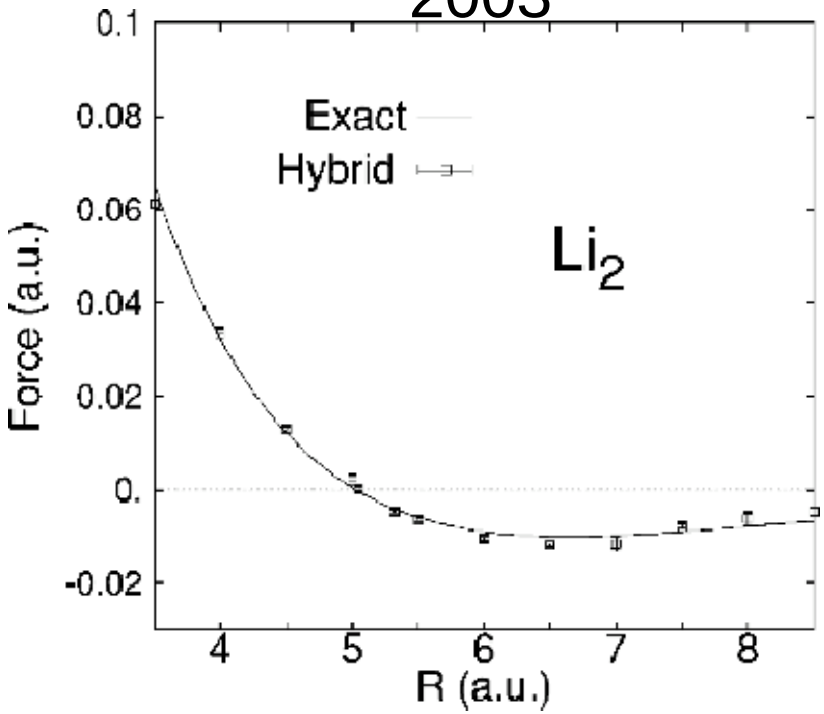

FIG. 11. Hybrid force for Li_2. Solid line: exact nonrelativistic force curve.

Lee, Mella, Rappe
2005

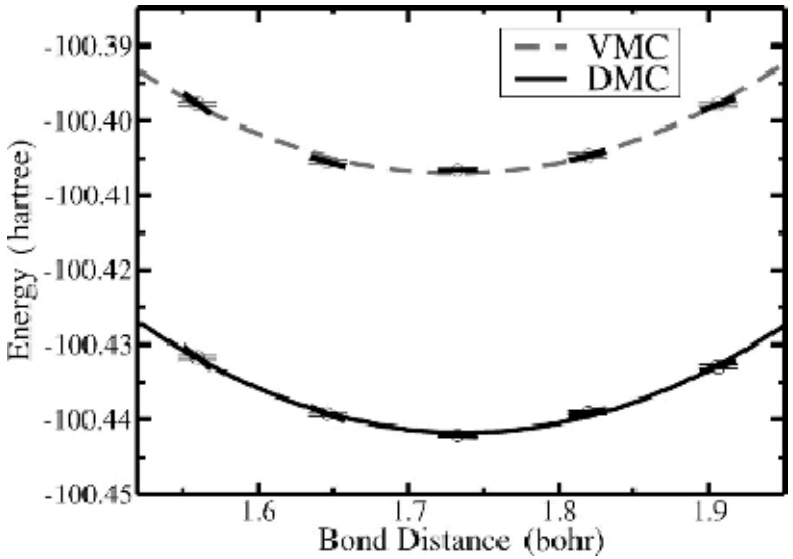

FIG. 1. Energy and force calculations of HF with VMC and DMC. Two thin horizontal lines at each data point show the energy error bar. The slope of the thick lines show the force at each data point.

improved estimators on the mixed distribution

Filippi, Umrigar 2000

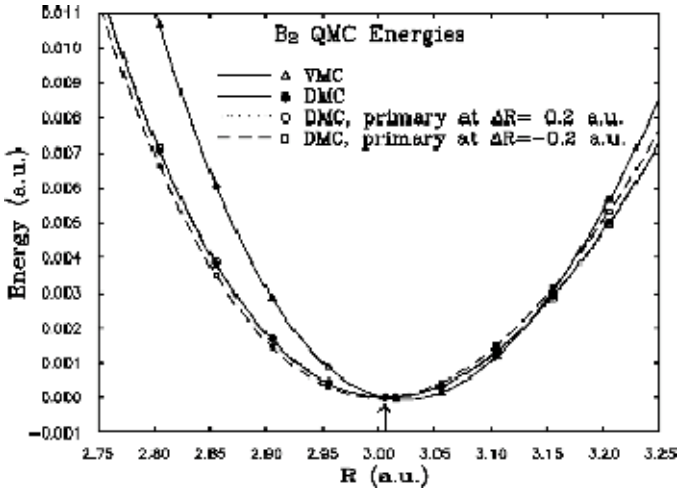

FIG. 2. Potential energy curve for B_2 in VMC and DMC. The three DMC curves are obtained with three different primary geometries (equilibrium, stretched by 0.2 and 0.2 a.u.) and using re-centered wave functions. All curves are shifted with the energy at the equilibrium distance (arrow) defined as the zero. Atomic units are used.

neglect contribution from drift-diffusion

Zong, Ceperley, 1998

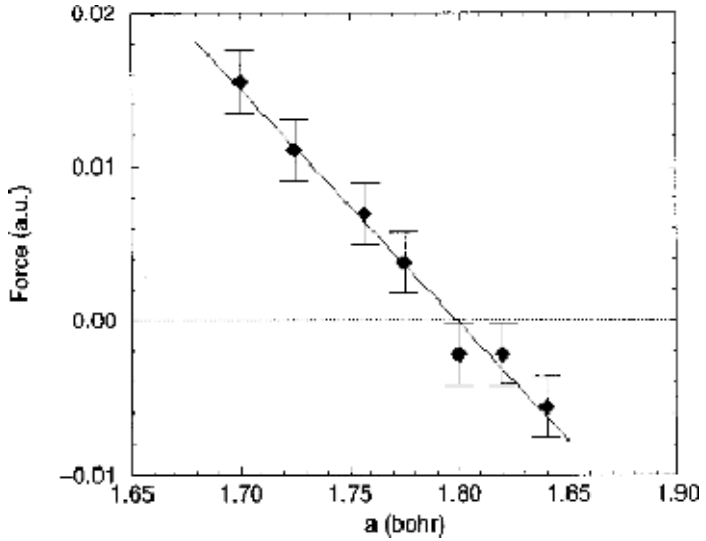

FIG. 6. The force on the outer protons in a H-H-H collinear configuration of H_3 molecule as a function of the nearest neighbor proton-proton distance a. Diamonds with error bars are PIMC simulations at $\beta = 38.4$ with 196 time slices. The solid line is a fit to the PIMC result.

neglect nodal displacement

J. Vrbik and S. M. Rothstein:

J. Chem. Phys., Vol. 96, No. 3, 1 February 1992

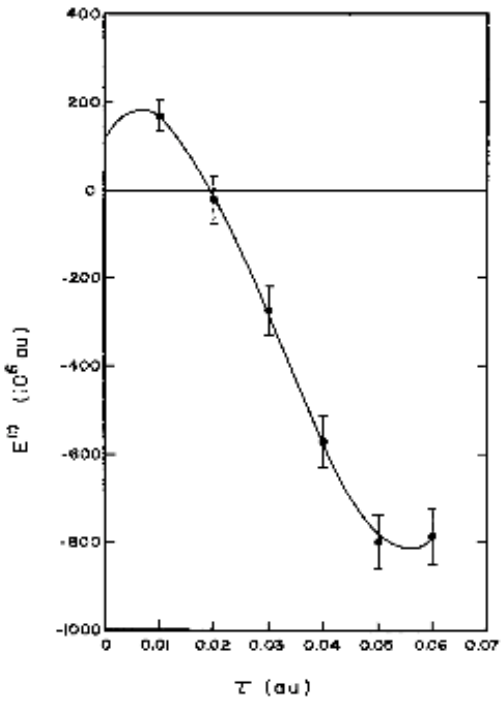

FIG. 1. Estimates of the first energy derivative [$E^{(1)}$ (a.u.)] vs time-step [τ(a.u.)] for the ground state of LiH at its equilibrium nuclear separation. Each point shown is the grand mean of twenty blocks using a τ-dependent truncation of the local energy and the b_k values and their derivatives. The curve shown is from a weighted polynomial regression.

includes everything

problems with time step extrapolation

Lithium dimer,
nodes from HF with STO3G basis

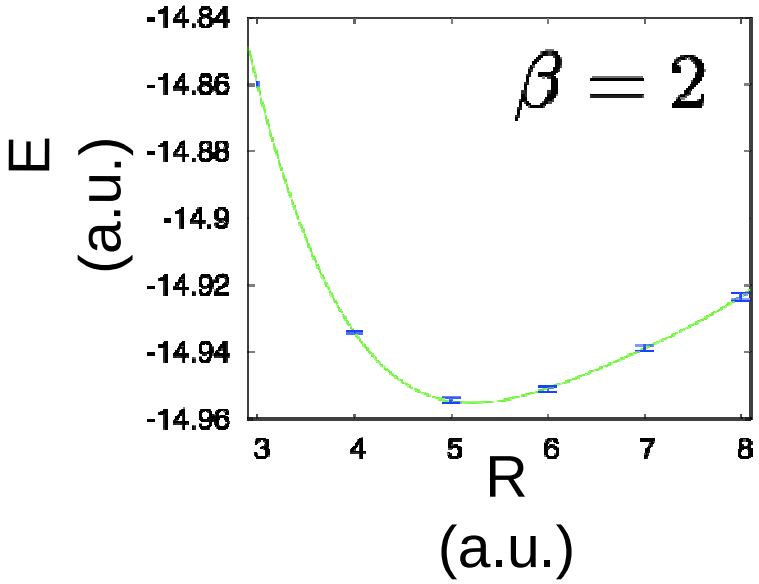

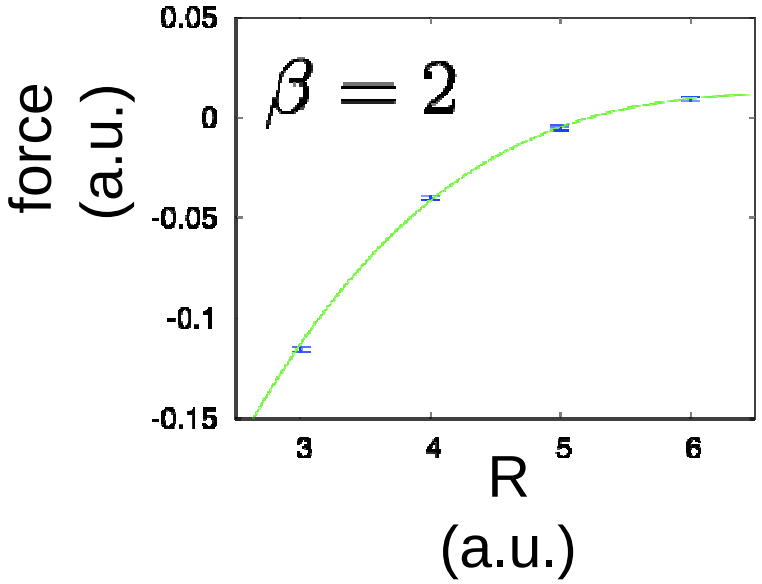

the force is consistent with the interpolation of E

scaling with: β

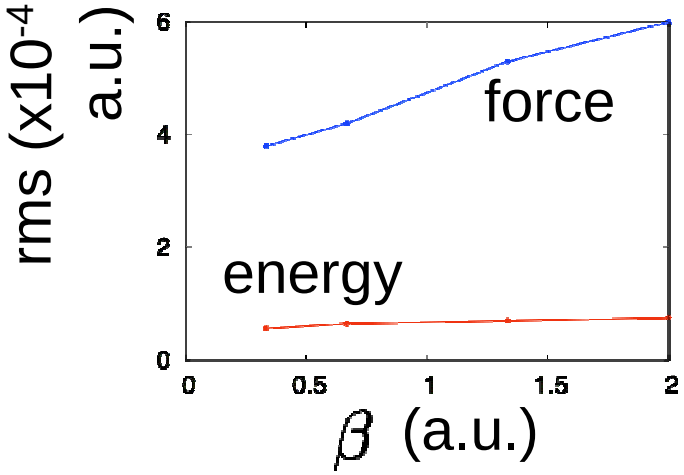

Dynamics: Free rotation in “superfluid” He clusters

The microscopic Andronikashvili experiment

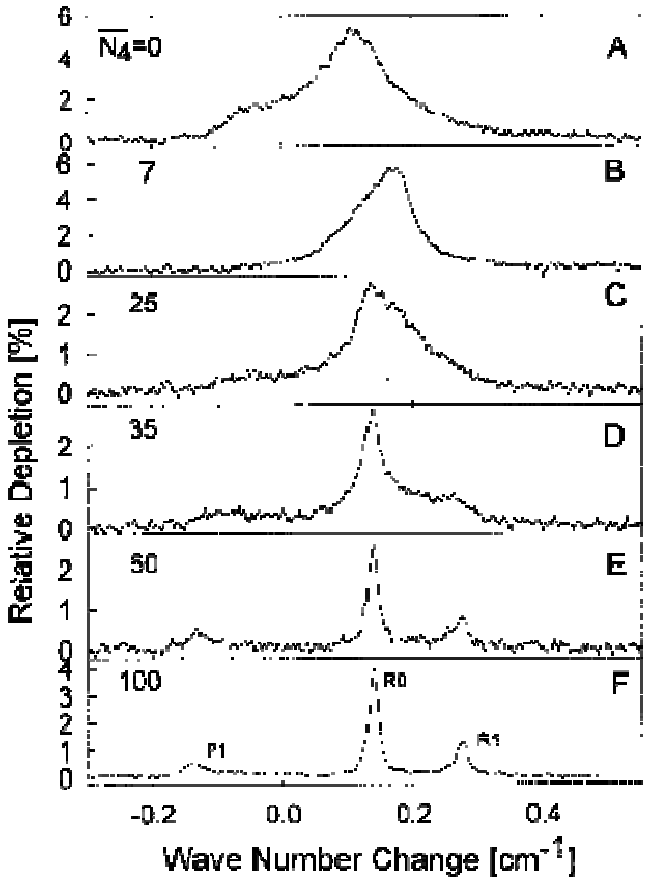

as few as ~60 ^{4}He atoms yield rotational peaks: “molecular superfluidity”

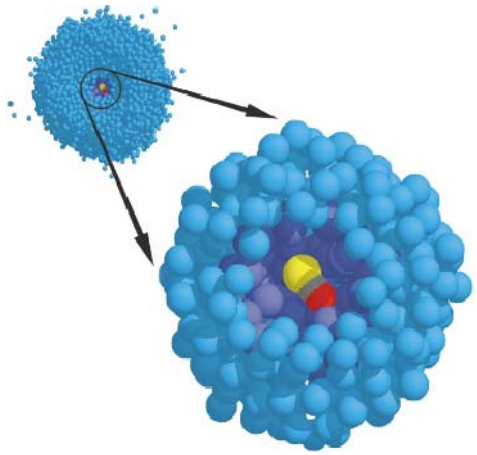

(S. Grebenev, P. Toennies, A. Vilesov, 1998)

size-selective measuremets in small clusters: OCS@He_N

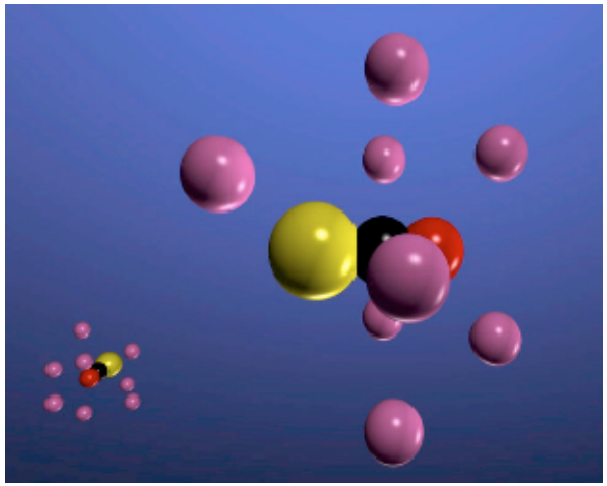

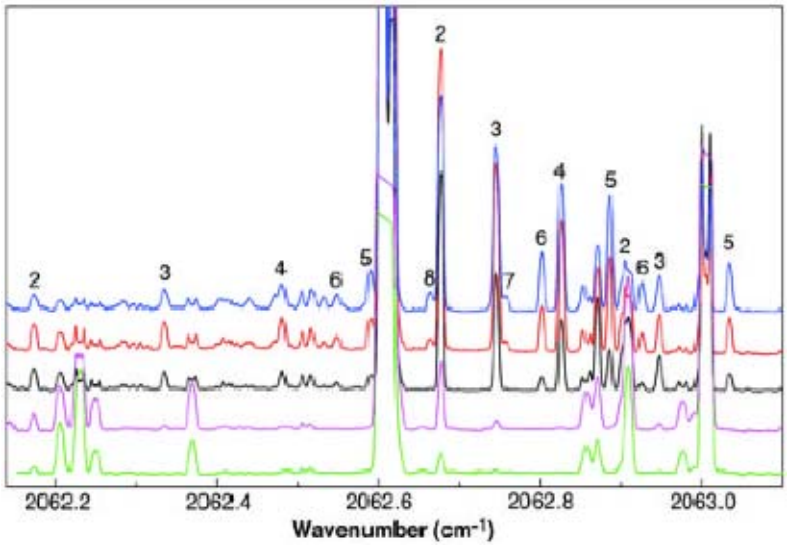

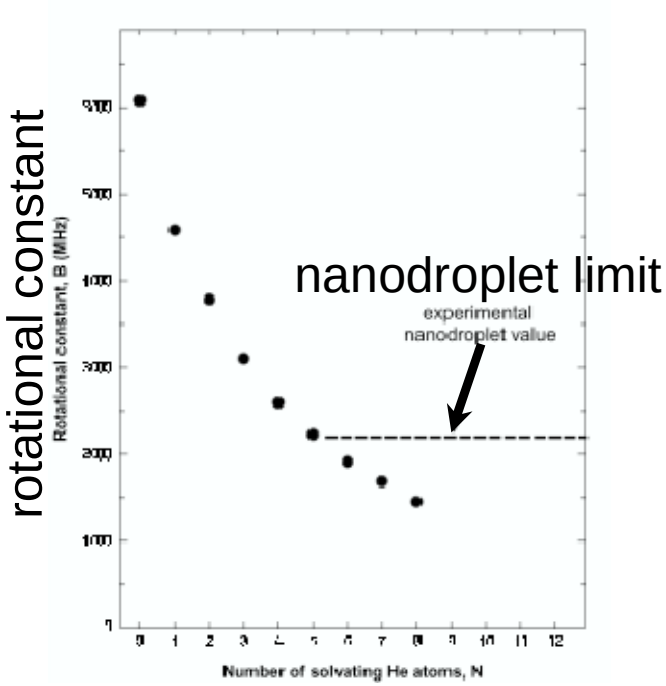

free-rotor-like IR and MW spectra assigned for N up to 8.

the rotational constant undershoots the asymptotic value for N=6, 7 and 8 thus implying a subsequent turnaround which will be taken as evidence for the onset of “superfluidity”

McKellar, Xu, Jaeger 2002

Calculating the optical spectrum

The measured absorption spectrum is

$$I(\omega) \propto 2\pi \sum_n |\langle \Phi_0 | \mathbf{d} | \phi_n \rangle|^2 \delta(E_n - E_0 - \omega) = \int e^{i\omega t} \langle \mathbf{d}(t) \cdot \mathbf{d}(0) \rangle dt$$

The dopant molecule is modeled as a rigid linear rotor interacting with He atoms with a pair potential.
The dipole **d** is proportional to the unit vector along the molecular axis.

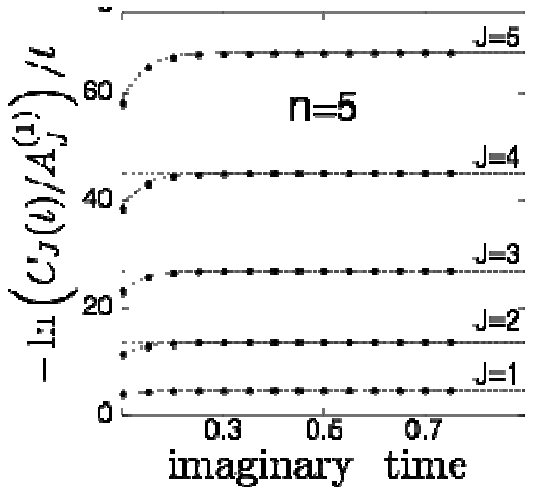

We can calculate correlation functions in imaginary time

$$C(t) = \frac{\langle \Phi_0 | \mathbf{d} e^{-tH} \mathbf{d} | \Phi_0 \rangle}{\langle \Phi_0 | e^{-tH} | \Phi_0 \rangle}$$

$$= \sum_n |\langle \Phi_0 | \mathbf{d} | \Phi_n \rangle|^2 e^{-(E_n - E_0)t}$$

Correlation functions of higher multipoles give higher-J states

$$C_J(t) = \langle P_J (\mathbf{d}(0) \cdot \mathbf{d}(t)) \rangle = \sum_n A_J^{(n)} e^{-(E_n - E_0)t}$$

Rotational excitation energies are obtained by inverse Laplace transform

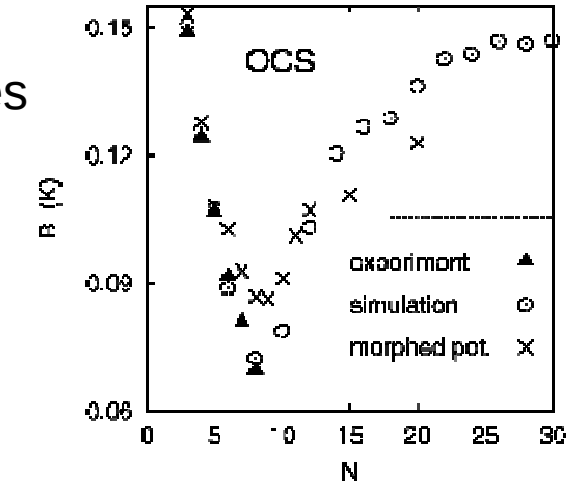

OCS@He$_N$: structure vs. rotational dynamics

He-OCS potential

He density profile

He-OCS angular correlation

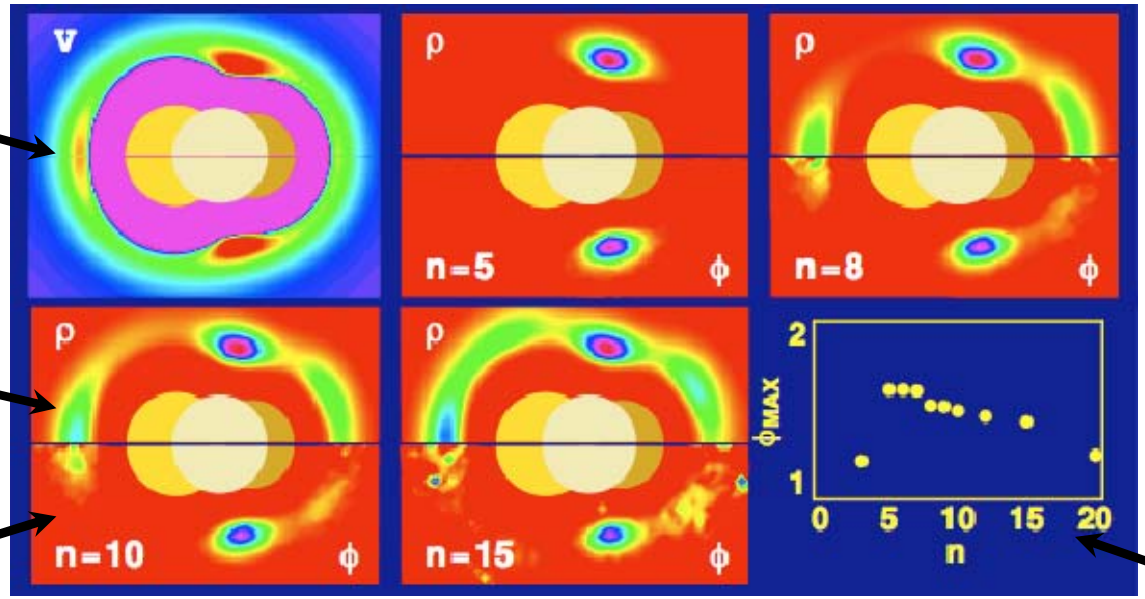

peak value of angular correlation

$$\rho(\mathbf{r}) = \langle \sum_i \delta(\mathbf{r} - \mathbf{r}_i) \rangle$$ He density

$$\phi(\mathbf{r}) = -\langle \mathbf{L} \cdot \mathbf{l}(\mathbf{r}) \rangle$$ He-OCS angular correlation

$$\mathbf{l}(\mathbf{r}) = -i\hbar \mathbf{r} \times \sum_i (\nabla_i \delta(\mathbf{r} - \mathbf{r}_i) + \delta(\mathbf{r} - \mathbf{r}_i \nabla_i)$$

HCCCN@He$_N$: MW spectra & QMC simulation

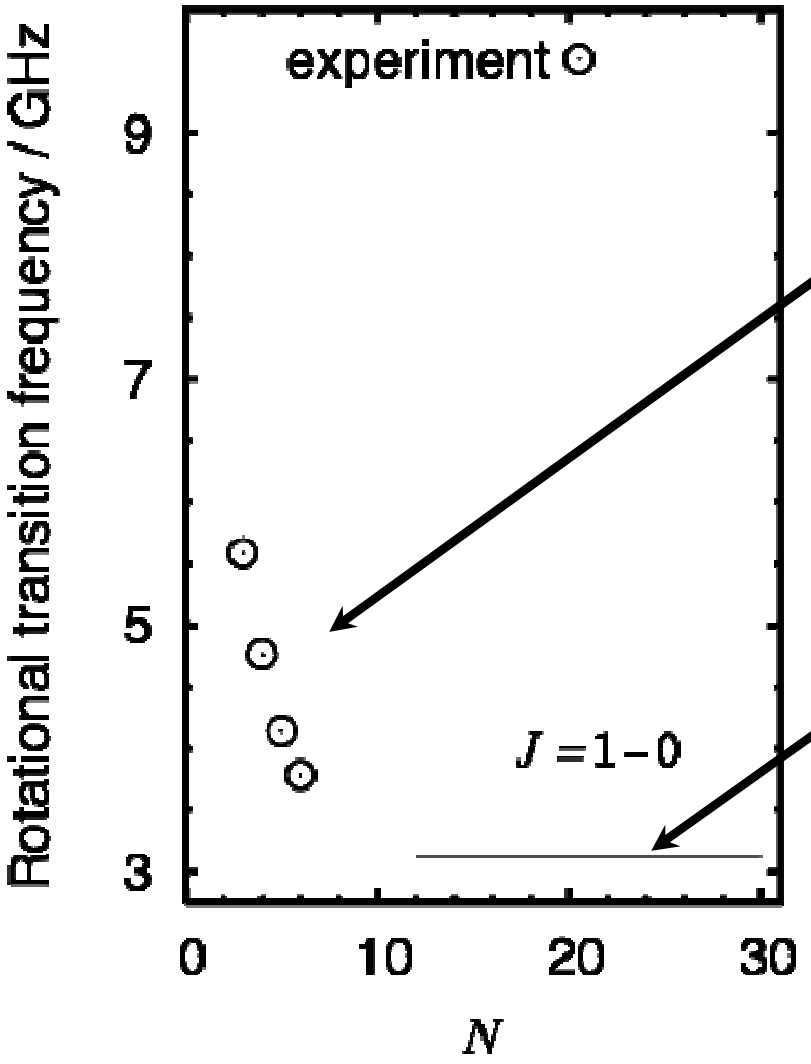

microwave transitions
(W. Topic and W. Jaeger, 2006)

nanodroplet limit
(Callegari et al.,2000)

HCCCN@He$_N$: MW spectra & QMC simulation

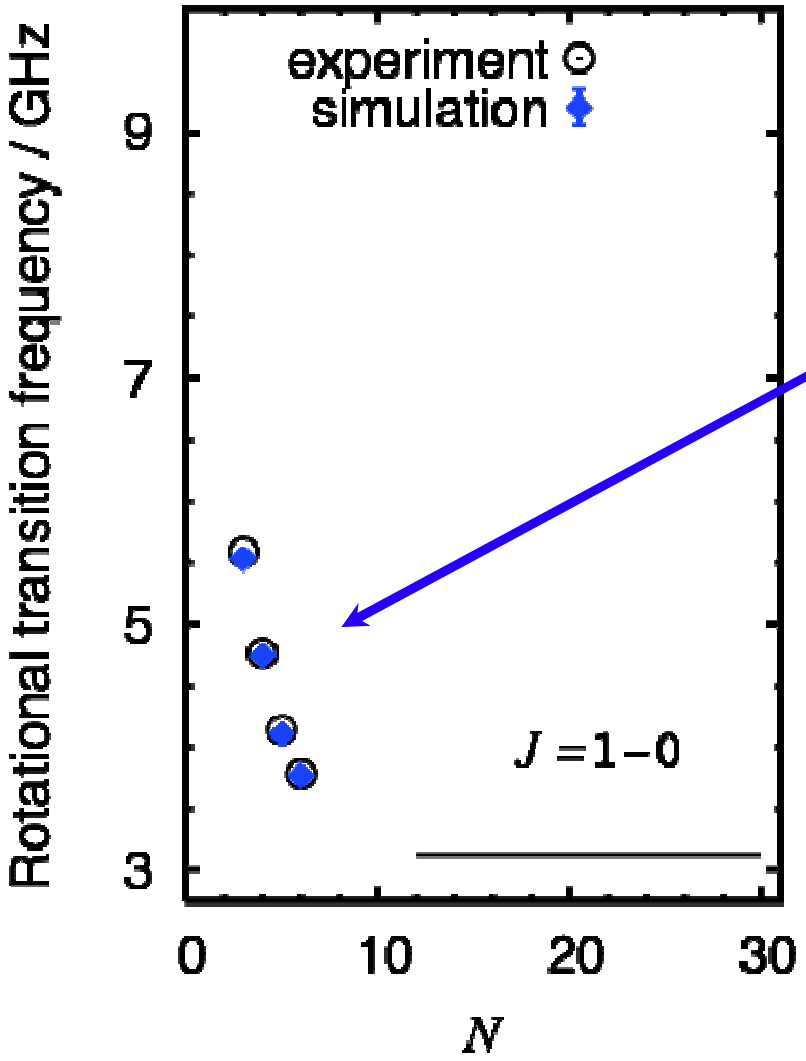

RQMC simulations

He-HCCCN potential

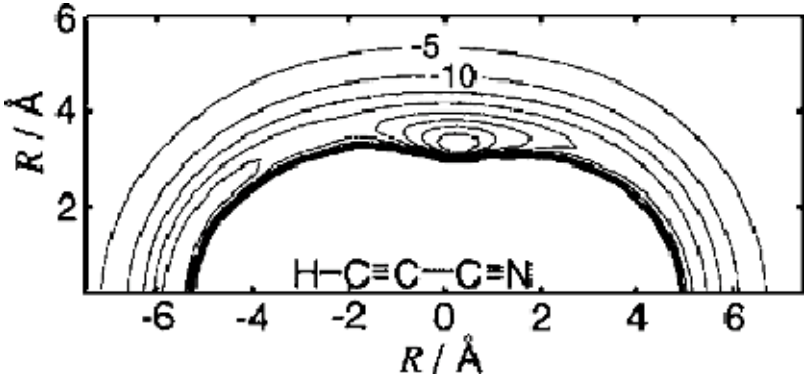

HCCCN@He$_N$: MW spectra & QMC simulation

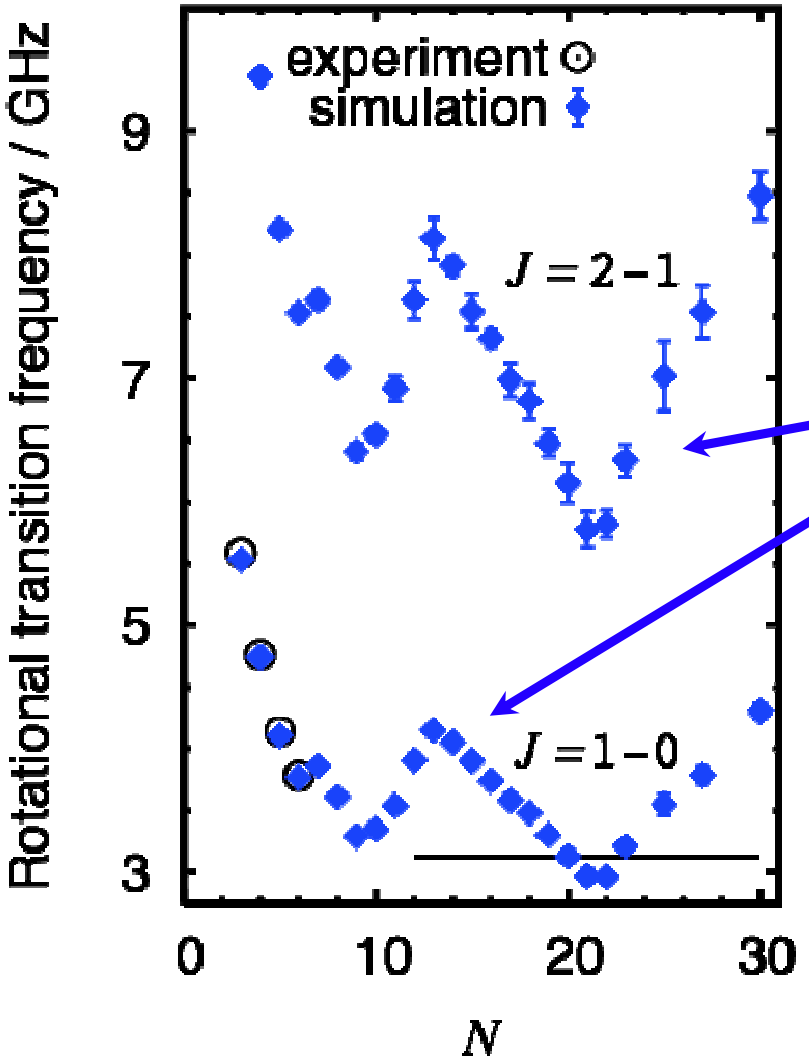

...more RQMC simulations

HCCCN@He$_N$: MW spectra & QMC simulation

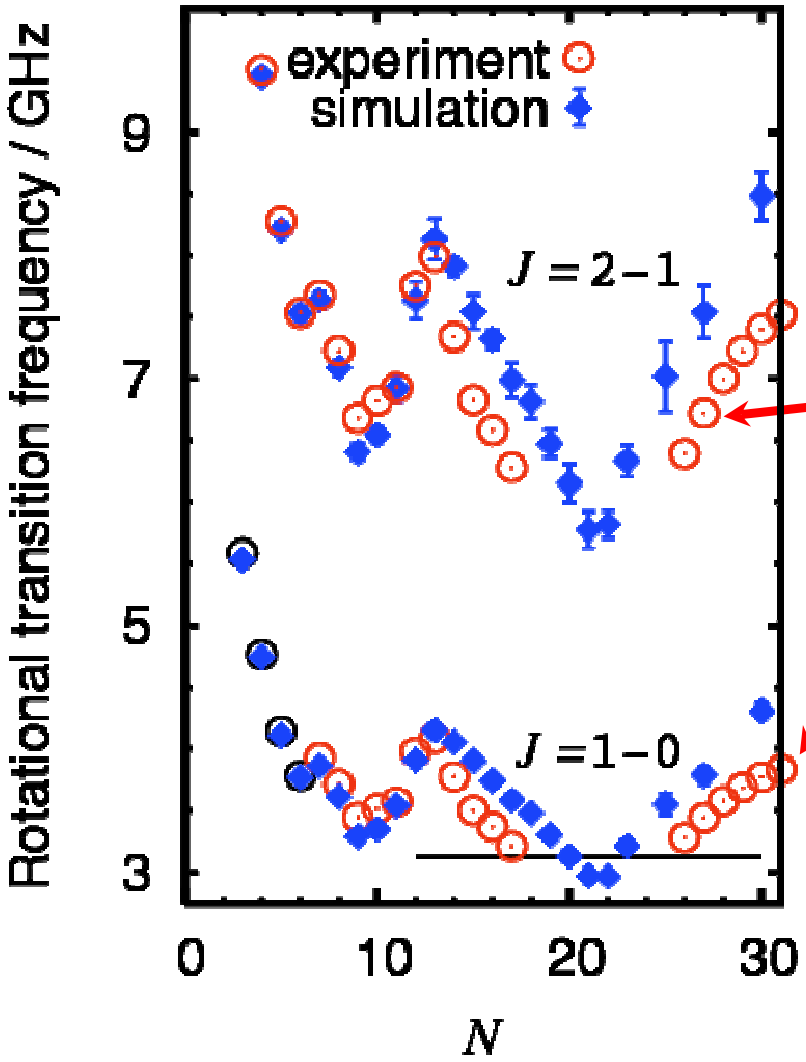

...more microwave transitions found and assigned with the help of computed rotational excitations

simulation facilitates the search and assignment of MW transitions

HCCCN@He$_N$: why local minima at 6 and 9 ?

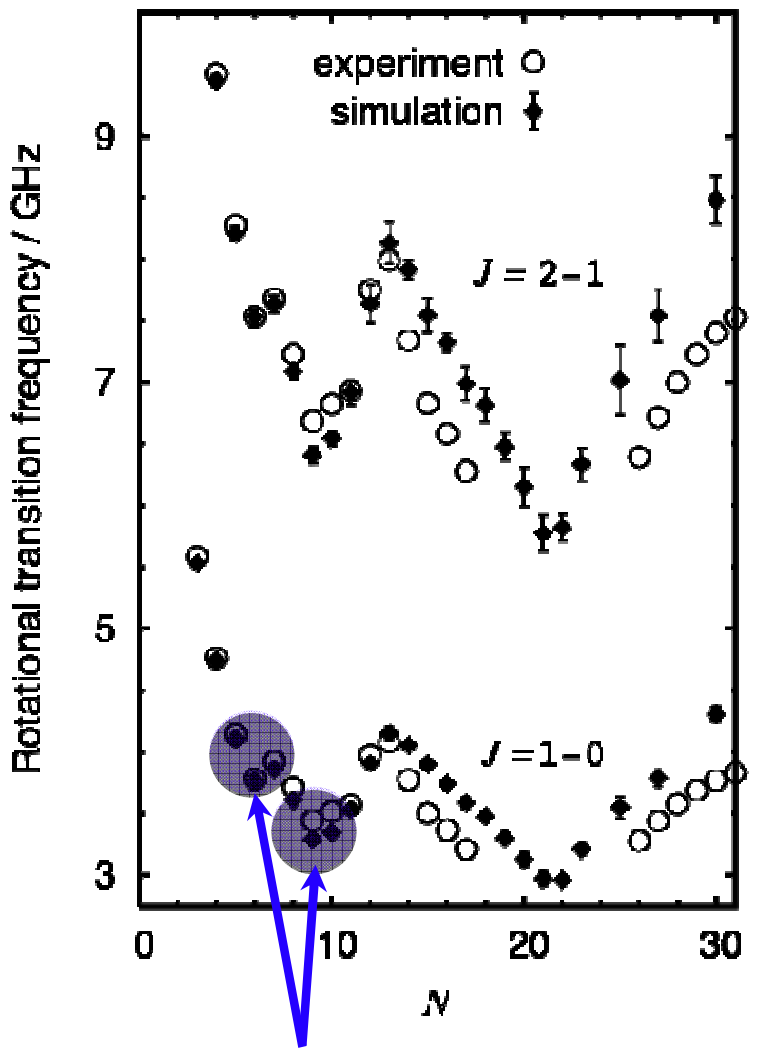

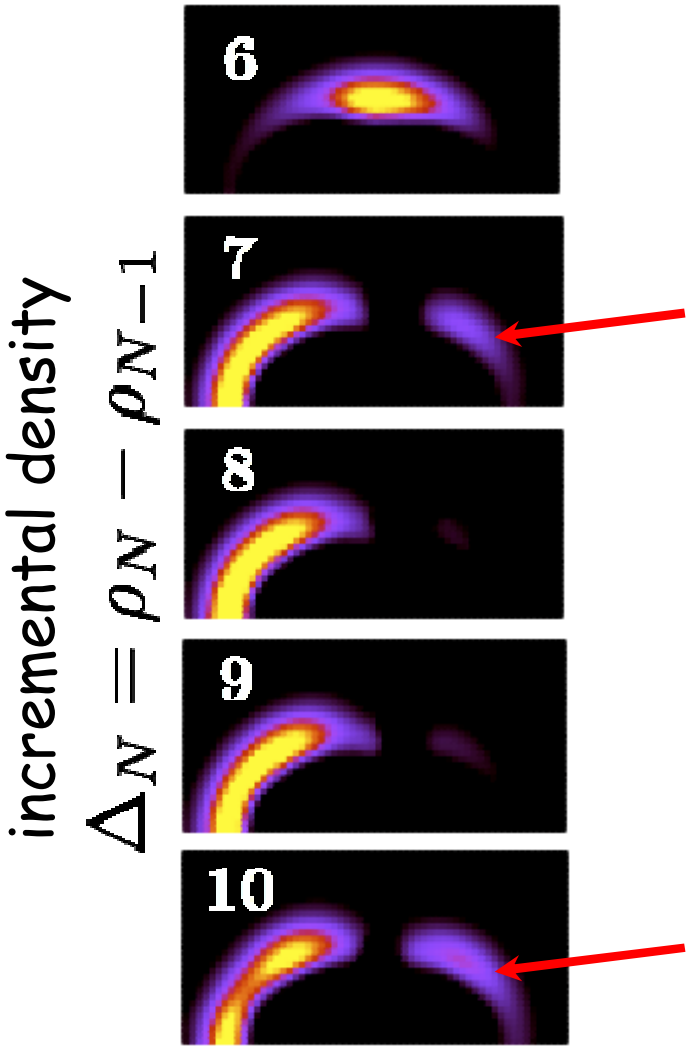

N=7 and 10 contribute to full solvation

HCCCN@He$_N$: why a local minimum at 22 ?

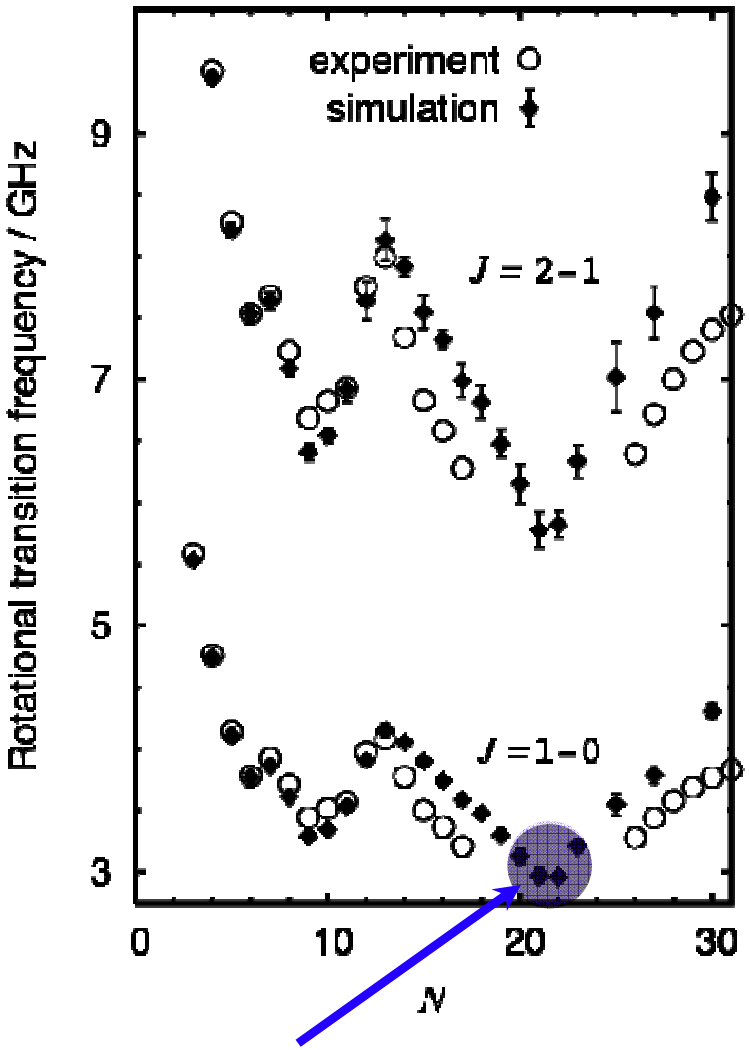

density profile

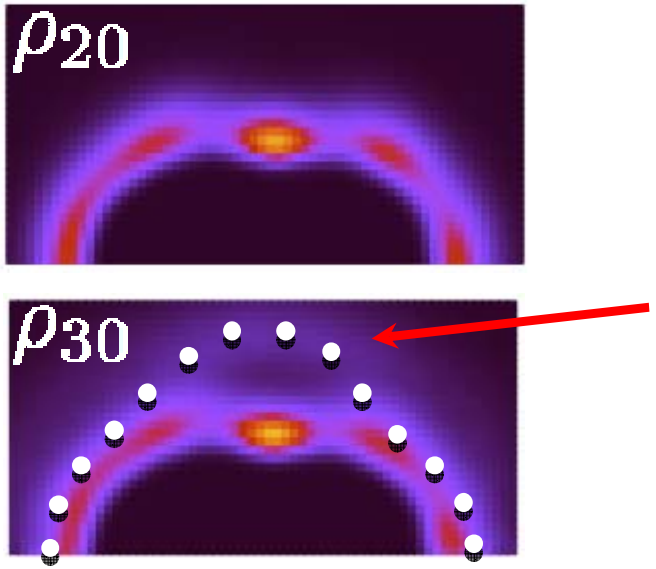

fraction of He atoms in long exchange cycles

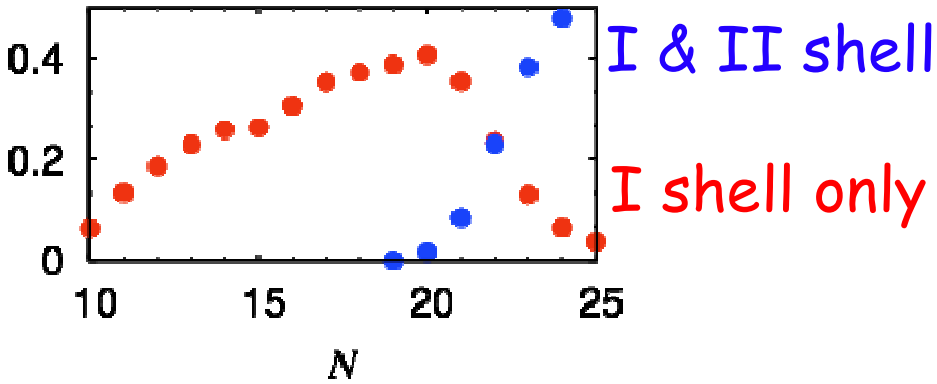

second shell opens new channel for exchange cycles

Introducing size scaling of efficiency:

Reminder

The practical utility of DMC relies on importance sampling.

- Rewrite the imaginary-time Schrödinger equation

$$\frac{1}{2}\nabla^2\Psi - V\Psi = \frac{\partial\Psi}{\partial\tau}$$

as an equation for $f(\mathbf{R},\tau) = \Psi(\mathbf{R},\tau)\Psi_T(\mathbf{R})$:

$$\frac{1}{2}\nabla^2 f - \nabla\cdot(\mathbf{v}f) - E_L f = \frac{\partial f}{\partial\tau}$$

where

$$\mathbf{v}(\mathbf{R}) = \frac{\nabla\Psi_T(\mathbf{R})}{\Psi_T(\mathbf{R})} \quad \text{and} \quad E_L(\mathbf{R}) = \frac{(-\frac{1}{2}\nabla^2 + V(\mathbf{R}))\Psi_T(\mathbf{R})}{\Psi_T(\mathbf{R})}$$

Projection Monte Carlo: Branching vs. Metropolis

Cost of calculating energies per particle vs. system size:
(VMC), DMC, ground-state Path Integral

4He at equilibrium density

Linear-Scaling Quantum Monte Carlo Calculations

A. J. Williamson, Randolph Q. Hood, and J. C. Grossman
Lawrence Livermore National Laboratory, 7000 East Avenue, Livermore, California 94550
(Received 3 May 2001; published 26 November 2001)

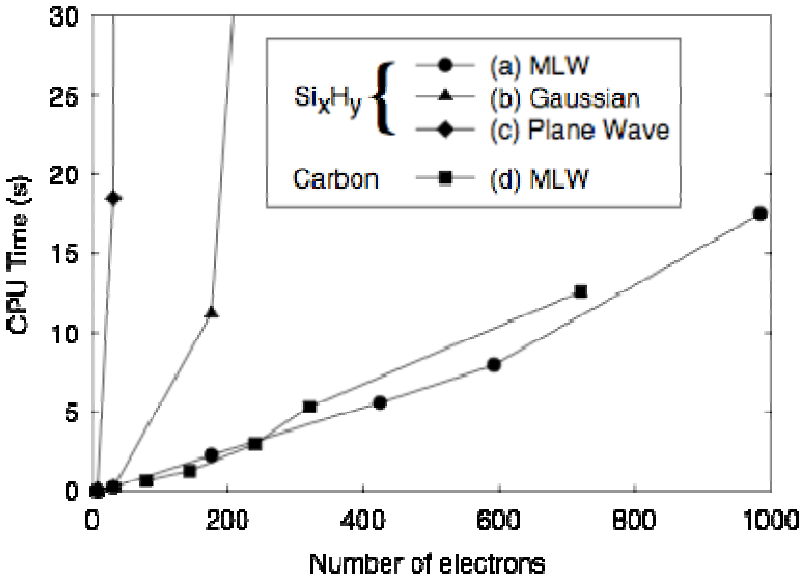

FIG. 2. CPU time on a 667 MHz EV67 alpha processor to move a configuration of electrons within DMC for SiH_4, Si_5H_{12}, $Si_{35}H_{36}$, $Si_{87}H_{76}$, $Si_{123}H_{100}$, $Si_{211}H_{140}$, C_{20}, C_{36}, C_{60}, C_{80}, and C_{180}.

Note, the discussion thus far involves the scaling of the computational cost of moving a single configuration of electrons. In practice, one calculates either (i) the *total* energy of the system, or (ii) the energy *per atom*, with a given statistical error. The statistical error, δ, is related to the number of uncorrelated moves, M, by $\delta = \sigma/\sqrt{M}$, where σ^2 is the intrinsic variance of the system. Typically, the value of σ^2 increases linearly with system size. Therefore, to calculate the *total* energy with a fixed δ, the number of moves, M, must also increase linearly. When multiplied by our linear increase in the cost of each move, an N^2 size scaling is obtained. For quantities *per atom*, such as the binding energy of a bulk solid, σ^2 still increases linearly with system size, but δ is decreased by a factor of N, and, hence, the number of required moves, M, actually decreases linearly with system size. Therefore the cost of calculating energies *per atom* is now independent of system size.

"cost of the move" extended to "cost of the calculation"

liquid ^{4}He at equilibrium density

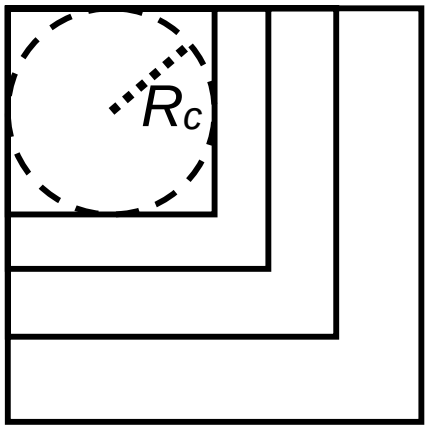

unit cell for
N = 64, 128, 256, 512

$$R_c = 7.15\text{Å}$$

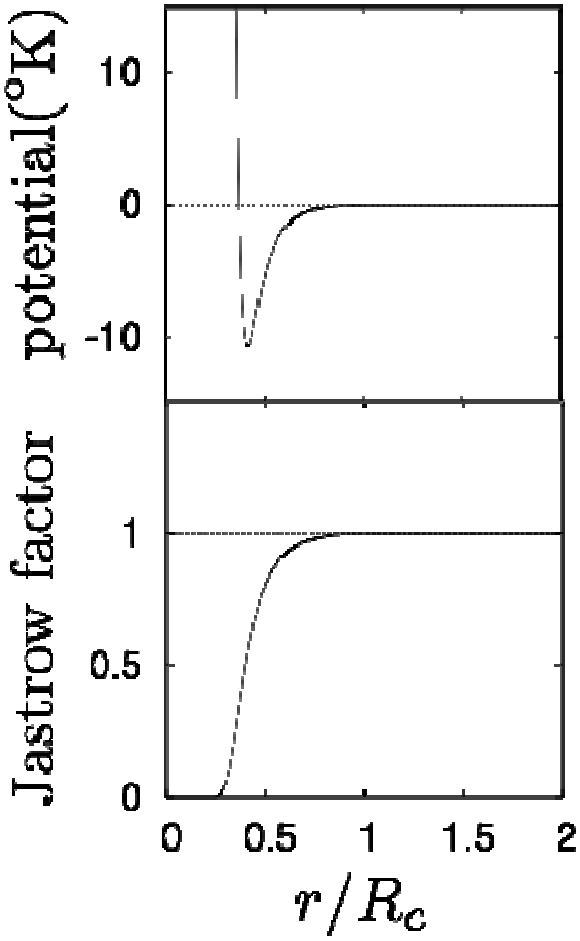

Aziz 79

McMillan

same potential
and wavefunction

Variational Monte Carlo

size effect:

energy
per particle

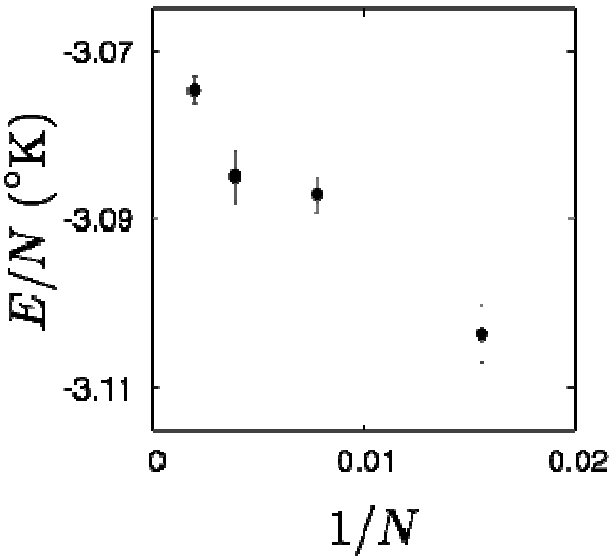

potential energy
per particle

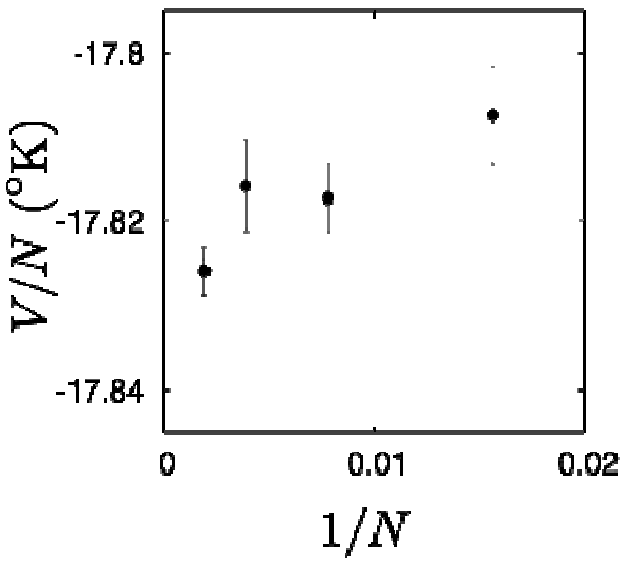

Variational Monte Carlo

variance of E_L
per particle

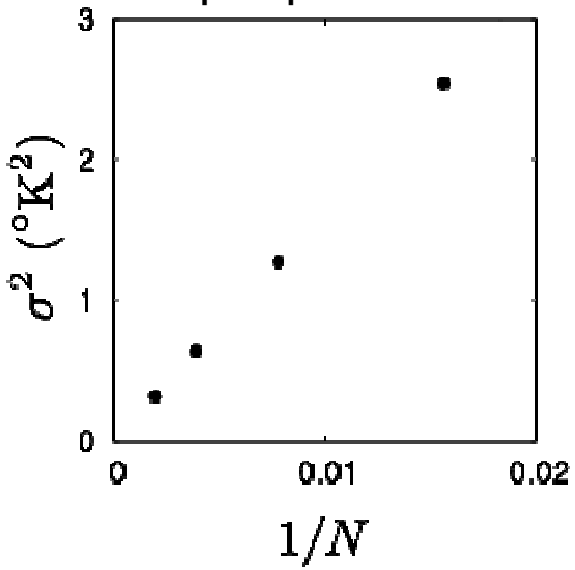

histogram of
E_L times DMC tstep

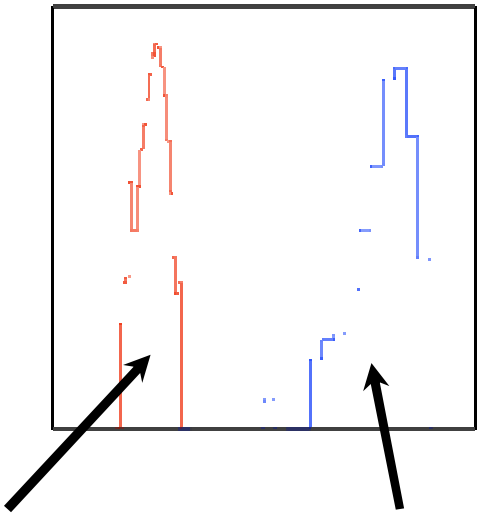

electron gas
N=54 r_S=10

4He
N=64

Variational Monte Carlo

variance of E_L
per particle

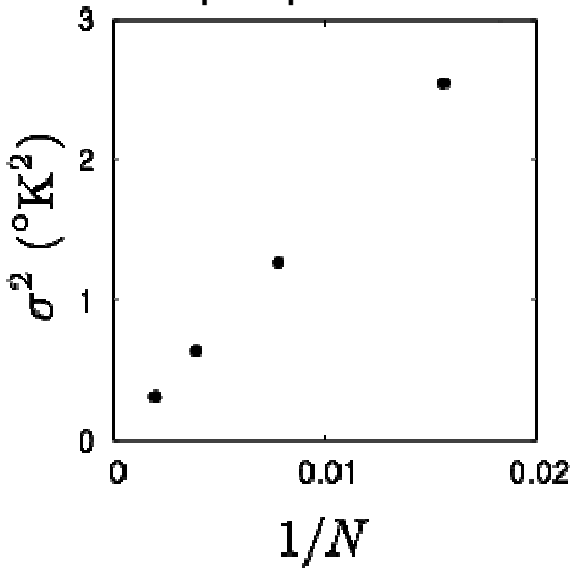

test function
for linear scaling

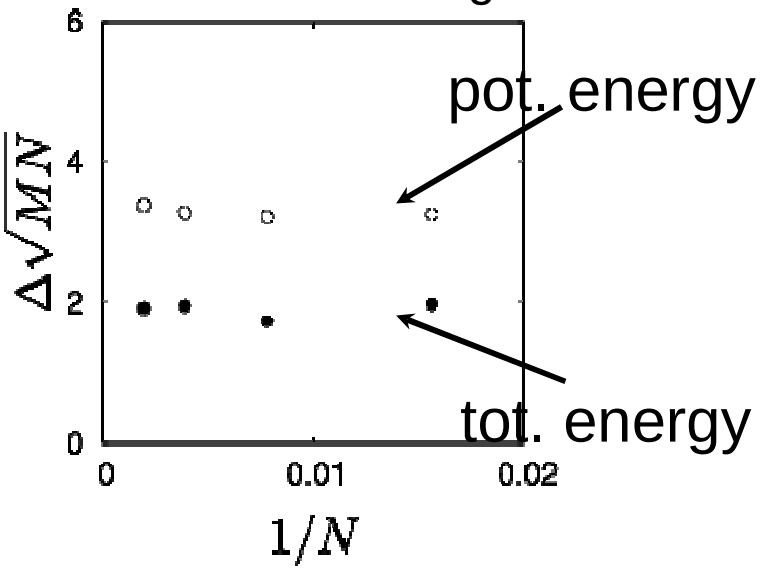

Δ statistical error

M number of steps

N number of particles

MN=T is the cost of the simulation
assuming linear scaling in the cost of the move. The efficiency is $\xi = 1/T\Delta^2$

ground-state Path Integral Monte Carlo

details of the simulation:

- primitive action:

$$\langle R|e^{-\tau H}|R'\rangle \simeq e^{-(R-R')^2/4\lambda\tau} e^{-\tau[V(R)+V(R')]/2}$$

- typical time step: $\tau = 10^{-3}K^{-1}$
- total projection time: up to $\beta = 2K^{-1}$ (2000 slices)
- multilevel Metropolis, bisection algorithm, level 6
  (attempt to move 63 slices, acc. rate about 50%, not necessarily optimal)

ground-state Path Integral Monte Carlo

results:

E vs. time step

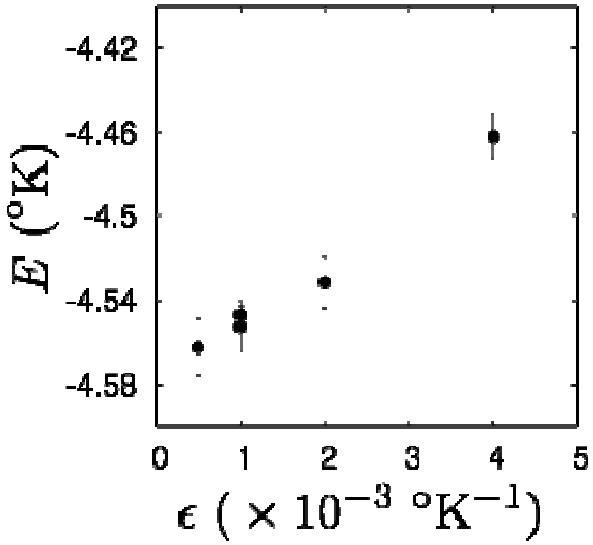

E vs. projection time

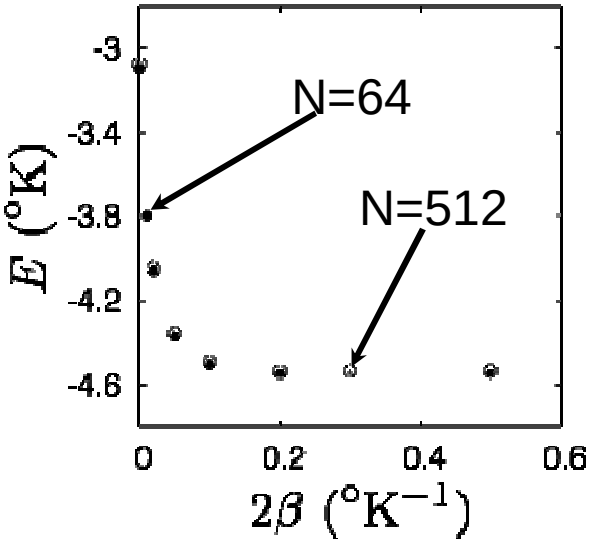

ground-state Path Integral Monte Carlo

test function
for linear scaling

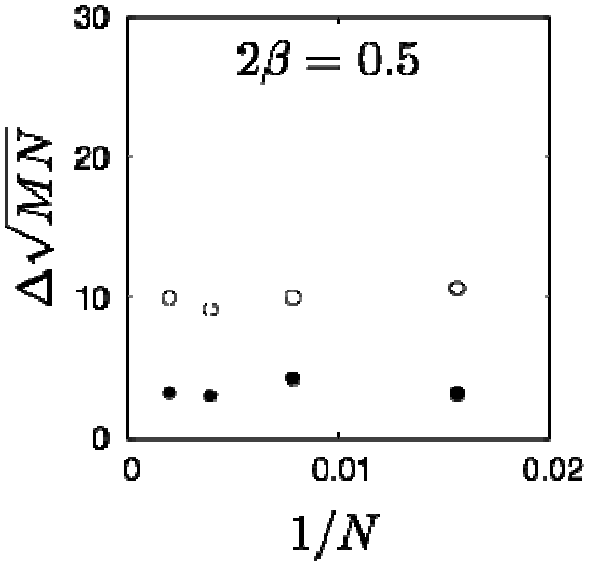

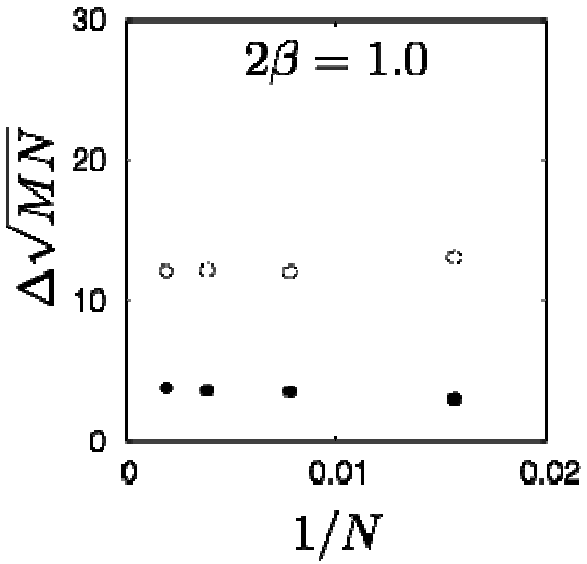

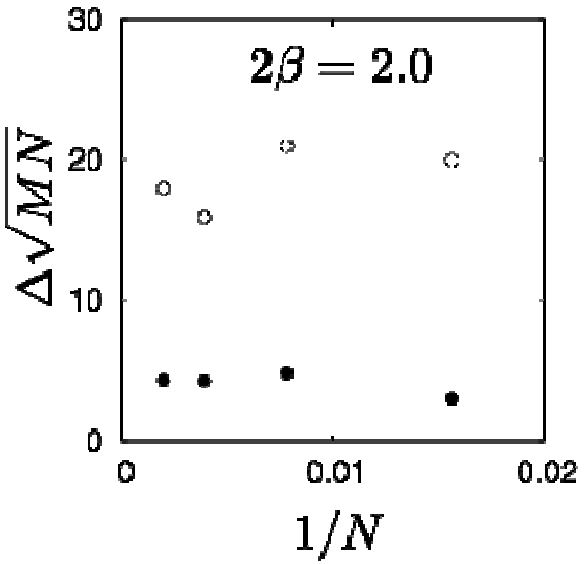

● total energy
○ potential energy

Δ statistical error
M number of steps
N number of particles

ground-state Path Integral Monte Carlo

test function
for linear scaling

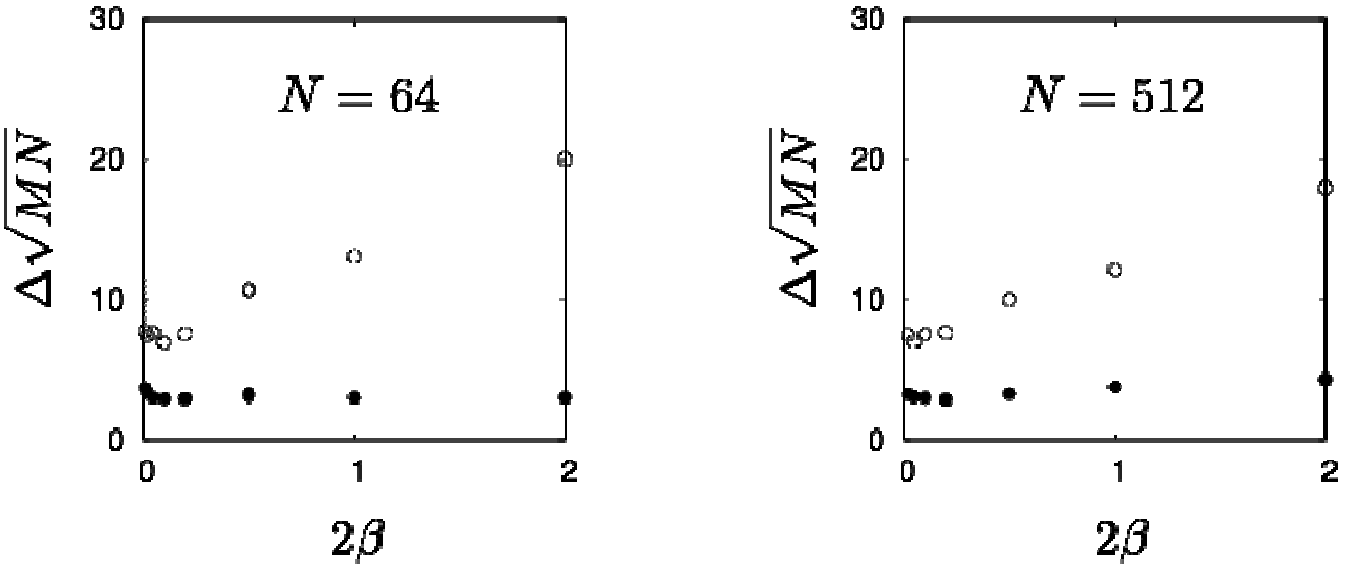

● total energy
○ potential energy

Diffusion Monte Carlo

$$f(R, t+\tau) = \int dR \tilde{G}(R, R', \tau) f(R', t)$$

$$\tilde{G}(R, R', \tau) \simeq e^{-(R'-R-2\lambda\tau V(R))^2/4\lambda\tau} e^{-\tau[E_L(R')+E_L(R)-2E_T]/2}$$

drift-diffusion

branching

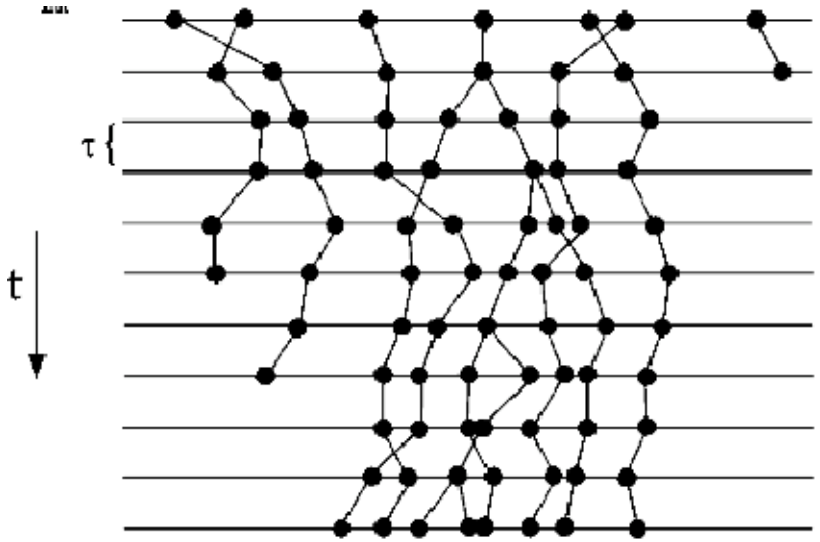

Diffusion Monte Carlo

details of the simulation:

- typical time step: $\tau = 10^{-3} K^{-1}$
- number of walkers: up to 8000
- branching is done (with constant number of walkers) after moving once all particles

Diffusion Monte Carlo

results:

time step error

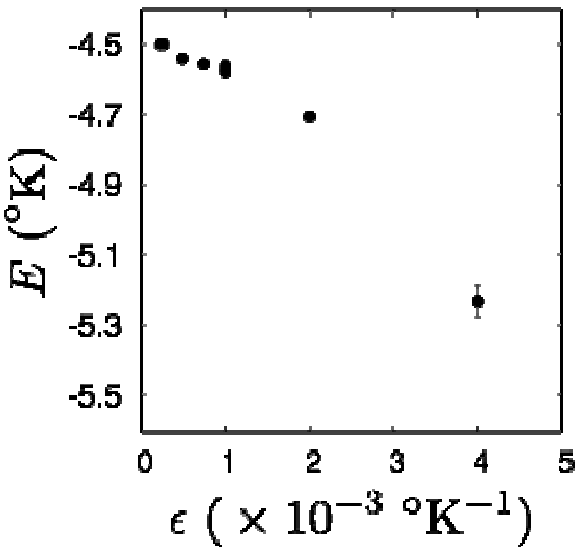

N=64

200 walkers

population control bias

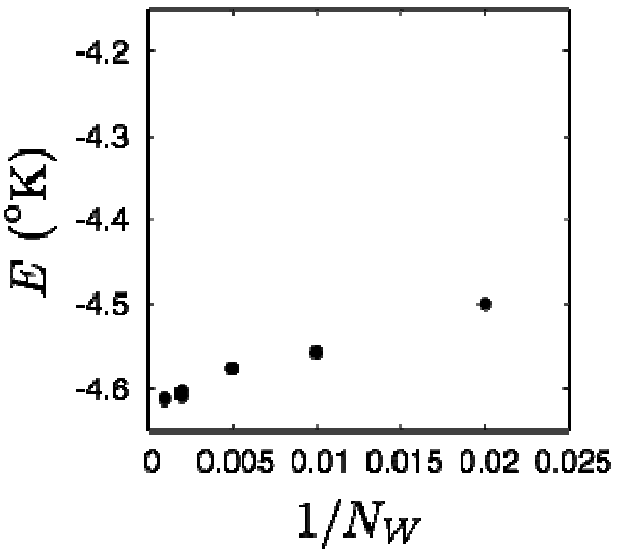

N=64

time step 0.001

Diffusion Monte Carlo

results:

time step error

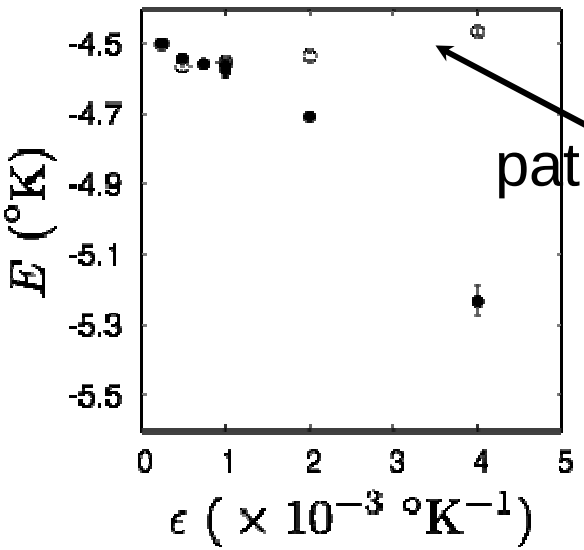

path integral

N=64

200 walkers

population control bias

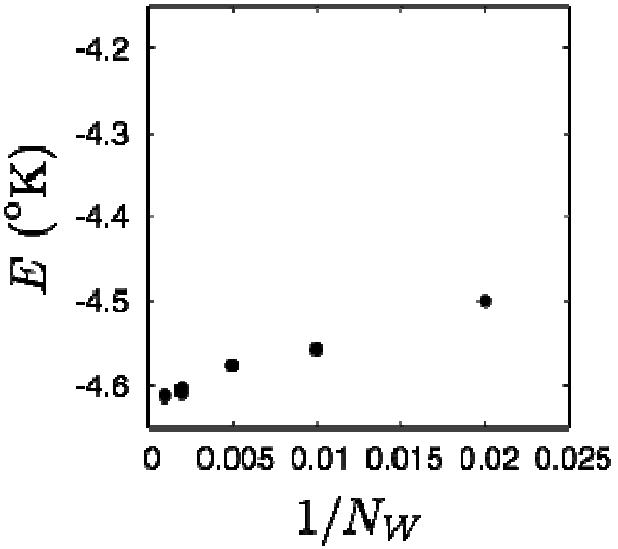

N=64

time step 0.001

Diffusion Monte Carlo

test function
for linear scaling

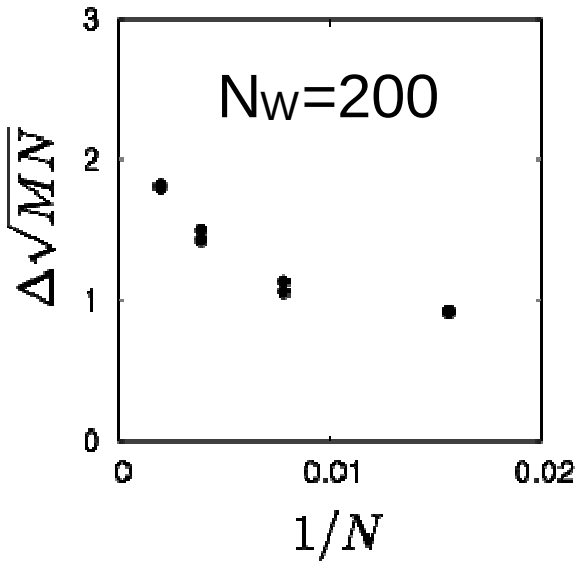

correlation between walkers increases
with system size

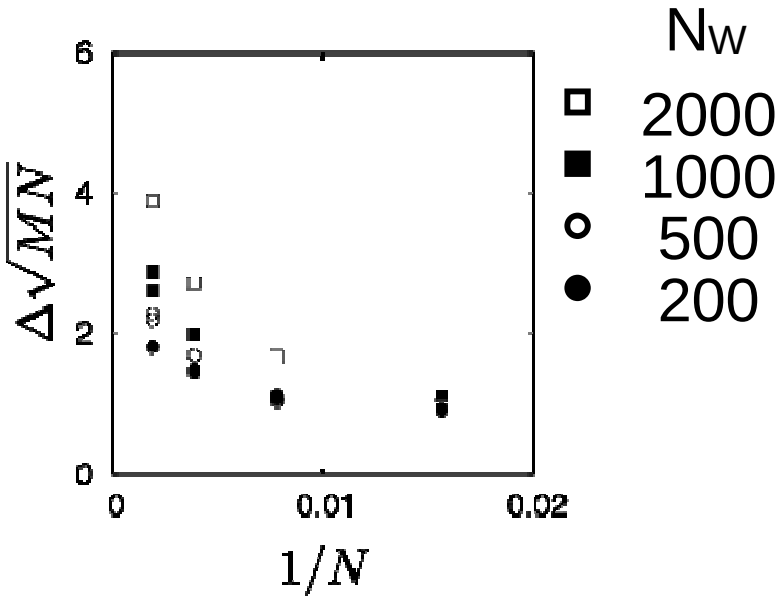

...and with number of walkers

Diffusion Monte Carlo

population control bias

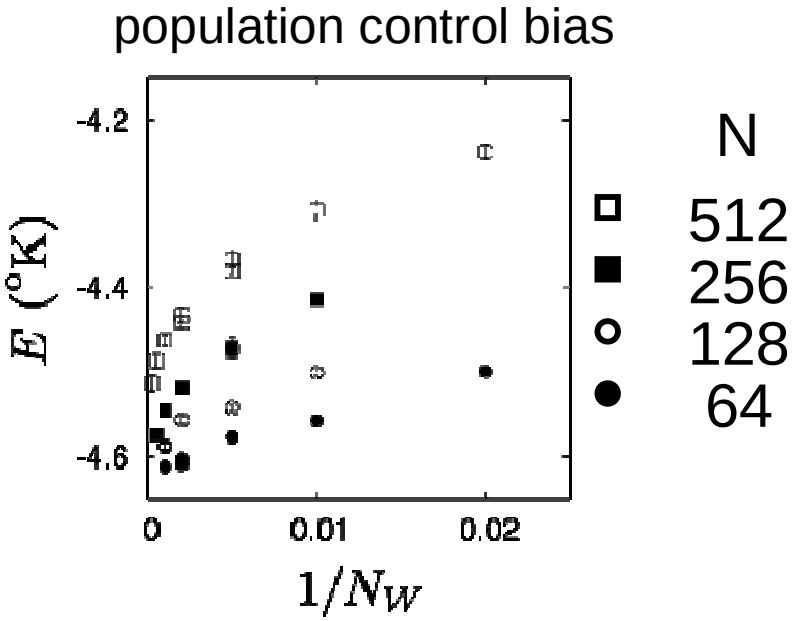

N

- 512
- 256
- 128
- 64

Diffusion Monte Carlo

population control bias

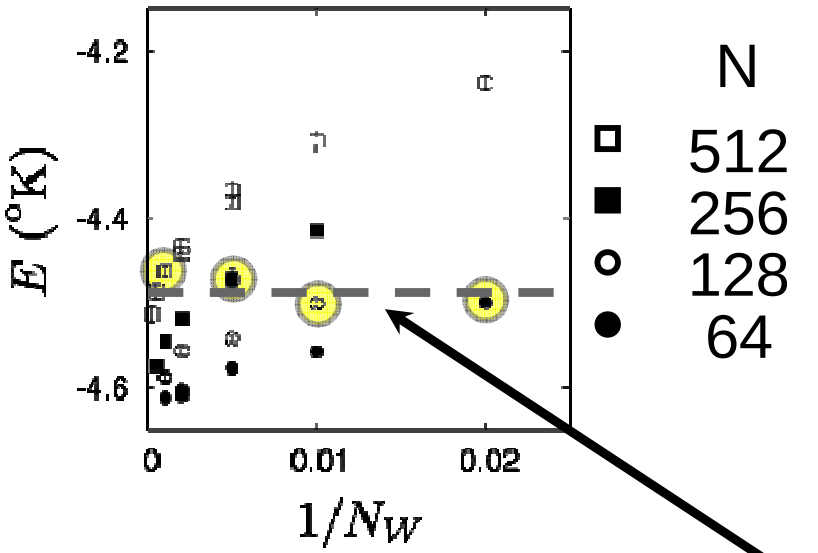

define a common level of systematic accuracy

Diffusion Monte Carlo

population control bias

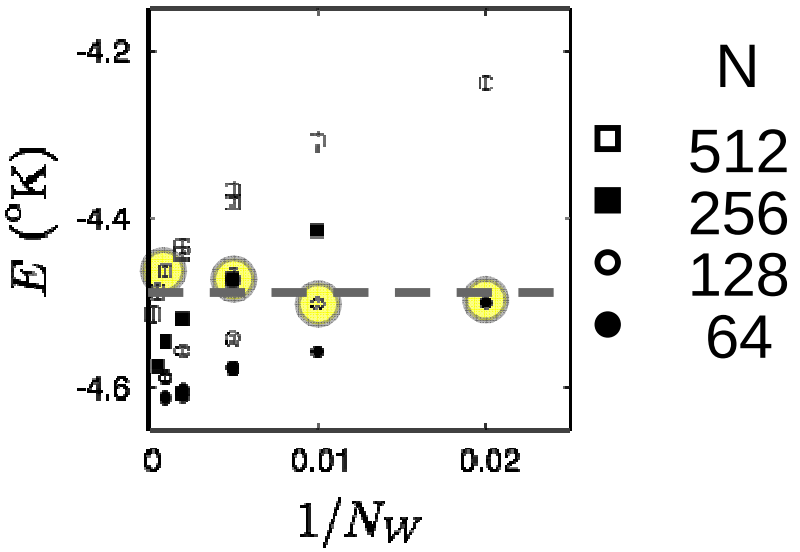

N
512
256
128
64

test function
for linear scaling

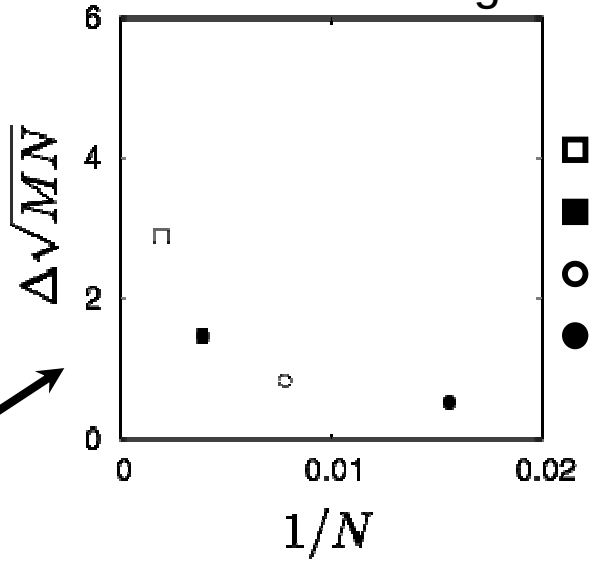

N_W
1000
200
100
50

estimate efficiency at similar level of systematic error

(worsens for higher accuracy)

Diffusion Monte Carlo

Eliminating the population control bias:

reweight the contributions of walkers at time *t* by the product of all renormalization factors of the total weight occurred since *t-T*

energy vs. correction time *T*

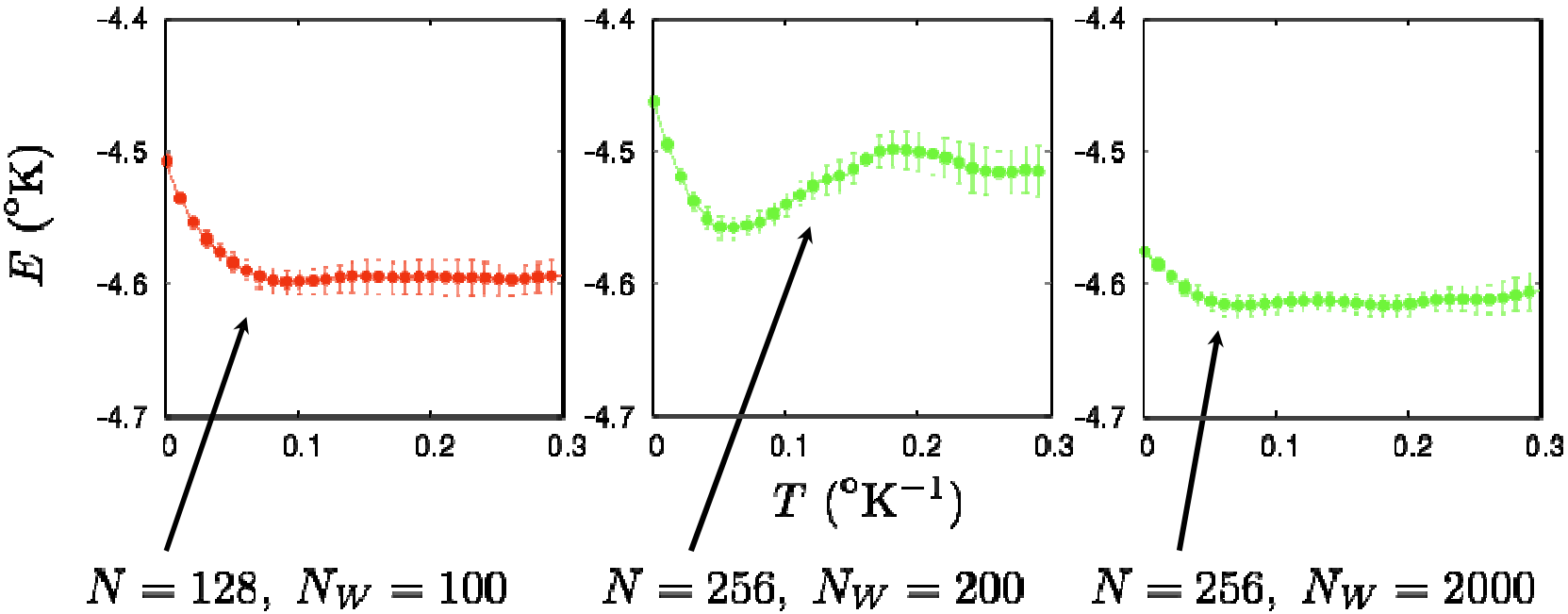

harder to get strong corrections for larger systems

Diffusion Monte Carlo

Eliminating the mixed estimate bias: Forward walking

a walker drawn from the mixed distribution at time t
contributes to the pure estimate the value of V of his ancestor at time t-T

recall path integral result:

E vs. projection time

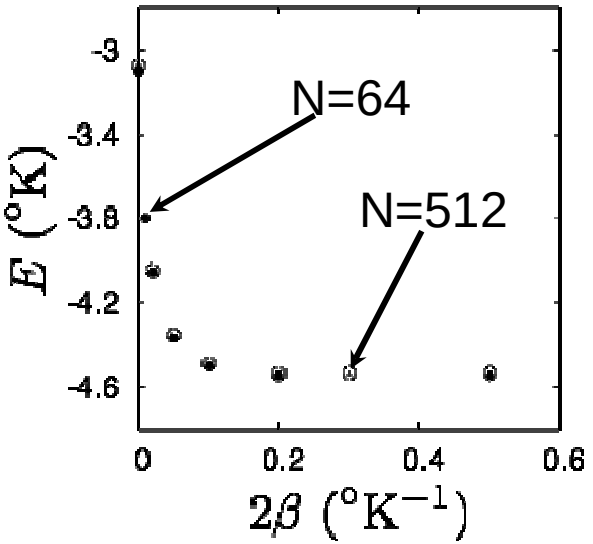

T should be about 0.15

Diffusion Monte Carlo

Eliminating the mixed estimate bias: Forward walking

$F_w(T)$ fraction of walkers with descendants after time T

$F_w(T=T_0)$ vs. N

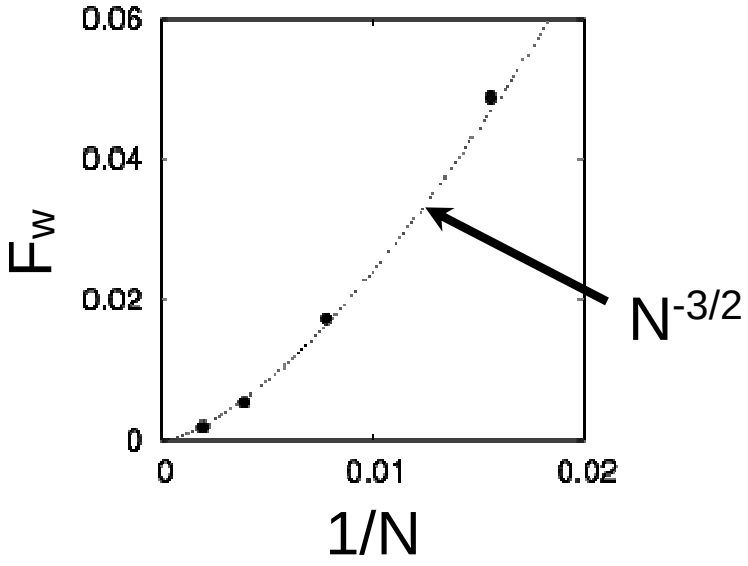

$T_0 = 0.15$

1000 walkers

$F_w \sim 1/T^3$

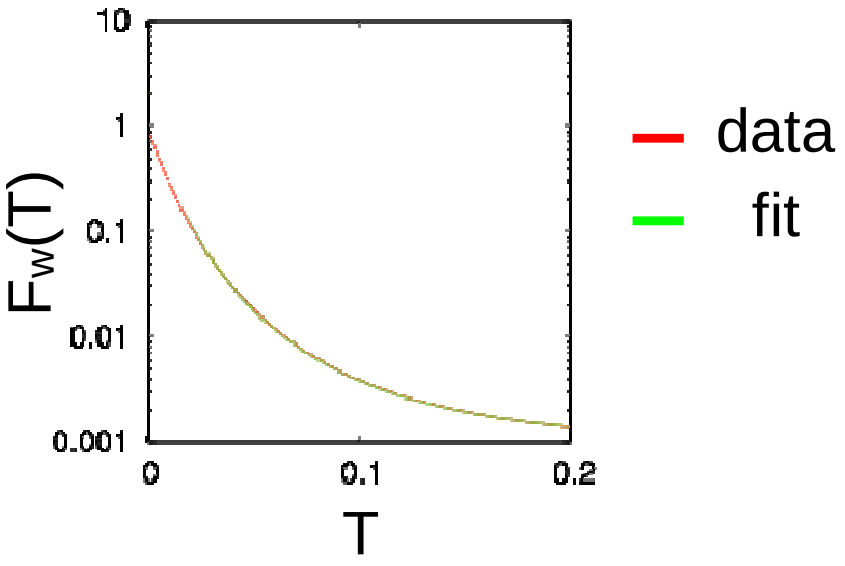

N = 512

1000 walkers

Diffusion Monte Carlo

Eliminating the mixed estimate bias: Forward walking

● forward walking alone

○ forward walking + eliminate population control bias

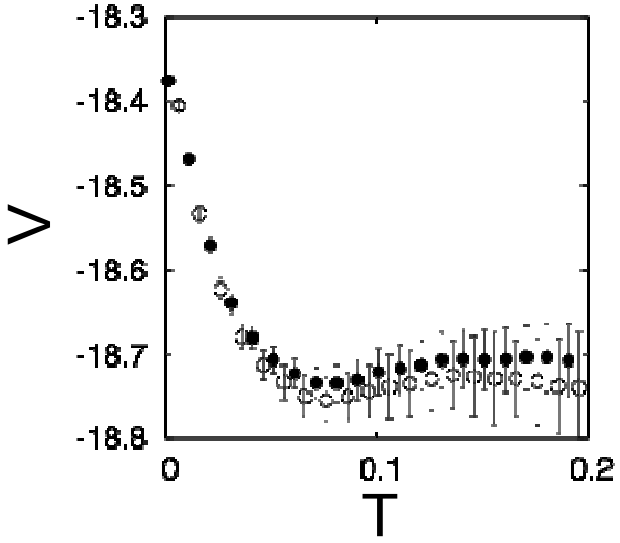

N=64

1000 walkers

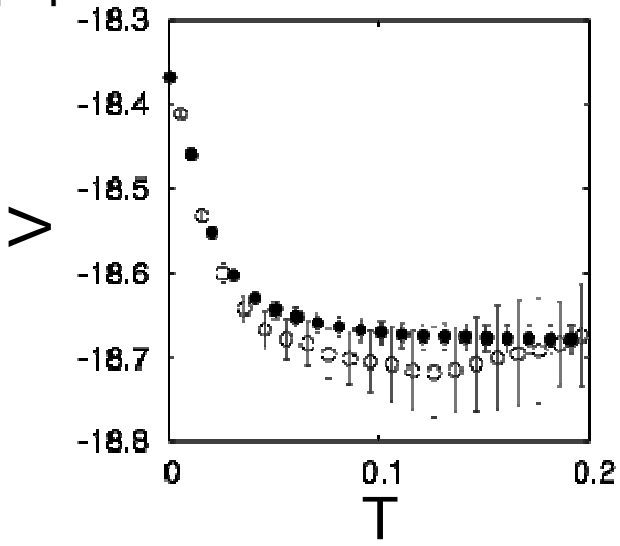

N=256

1000 walkers

Diffusion Monte Carlo

Eliminating the mixed estimate bias: Forward walking

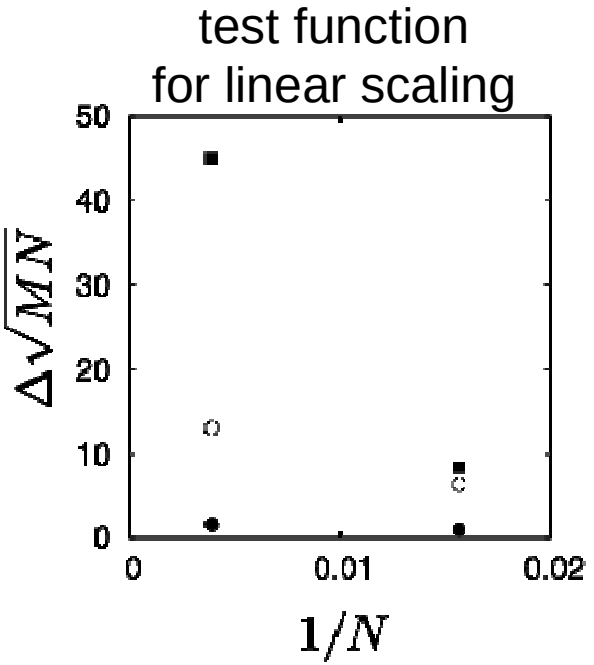

■ unbiased
○ forward walking
● mixed estimate

- for large systems and/or poor trial functions branching becomes problematic

- PIMC scales in a controlled way; for condensed helium the DMC/PIMC efficiency crossover is at sizes of practical interest

- PIMC does not (necessarily) heavily rely on the quality of the trial function (except for FN approx.)

- as a Metropolis algorithm it can be improved introducing better moves

- it is more straightforward for derivatives, imaginary-time correlations, correlated sampling...